Offset rivers, drainage spacing and the record of strike-slip faulting:

the Kuh Banan Fault, Iran

Faye Walker*, Mark B. Allen

Department of Earth Sciences, University of Durham, Durham, DL1 3LE, UK

*Corresponding author.

e-mail: fayemousw@googlemail.com; m.b.allen@durham.ac.uk

ABSTRACT

This study concerns the ways in which rivers can record part, but not necessarily all, of strike-slip fault offset. The focus is the active right-lateral Kuh Banan Fault in eastern Iran, within the Arabia-Eurasia collision. Plate convergence has caused thrust and strike-slip faulting across SW Asia. The active slip rate of the Kuh Banan Fault is ~1-2mm/yr. Total displacement is ~5-7 km, as determined from offset geological markers and the length of a pull-apart basin. A component of thrusting has generated ~1 km of relief, which preserves the offset of rivers displaced laterally by the strike-slip motion. Ridge half-widths (W), and river outlet spacings along the fault (S) are related by the drainage spacing parameter R, where $R = W/S$. Published data for older, larger mountain ranges have extremely characteristic drainage spacing ($R = 2.1$). Drainage spacing along the Kuh Banan Fault has a mean value of 1.8 and is much more variable ($R = 1.1\text{-}3.1$), due to local structural complexities which have influenced river courses. Most river offsets along the Kuh Banan Fault are small (<100 m); the maximum observed offset (~3.5 km) is smaller than the total fault displacement of at least ~5 km. The most likely explanation for this discrepancy is stream capture, whereby reaches of rivers downstream of the fault are juxtaposed by fault slip against rivers upstream of the fault. In this way, offset of individual rivers is repeatedly reset to zero. Stream capture is influenced by outlet spacing such that the largest rivers can accumulate large offsets, while smaller, closely

1

spaced rivers are captured more often, inhibiting large offsets. The mean offset of the main rivers along the Kuh Banan Fault is one-third their mean drainage spacing, indicating that the spacing of smaller rivers controls the size of the maximum offset.

Keywords: strike-slip fault; river offset; Iran.

1. Introduction

Deformation within tectonically active regions has significant effects on river systems. Strike-slip faulting can result in the lateral offset of rivers, as well as other geological and geomorphic markers (Huang, 1993; Fu *et al.*, 2005; Fu & Awata, 2007; Cowgill; 2007; Cowgill *et al.,* 2009), while uplift causes incision and may result in the deflection of river channels, affecting drainage basin geometry. The pattern of stream offsets along a strike-slip fault can provide clues about its movement and the growth of fault-related topography and how this affects drainage development (Fu *et al.*, 2005; Jackson *et al.*, 1996). Offsets along strike-slip faults are known to increase with time due to repeated slip (Sylvester, 1988) so that the largest observed offset should equal the total fault displacement. This is generally thought to be the case for offsets of large rivers as well as more permanent geological markers (e.g. Westaway, 1994; Talebian & Jackson, 2002; Fu *et al.*, 2005; Fu and Awata, 2007). It is also possible to restore multiple smaller offsets (by matching channels on either side of the fault and finding the best-fitting configuration) to determine the total fault displacement, as has been shown for the Red River Fault in east Asia (~25 km offset; Replumaz *et al.*, 2001).

It has long been observed that there is a remarkable degree of regularity in the spacing of river outlets along mountain fronts, particularly in linear mountain ranges where the drainage runs transverse to the mountain front (Hovius, 1996; Talling *et al.*, 1997; Purdie & Brook, 2006). Hovius (1996) developed a quantitative method for documenting the regularity of drainage spacing in large-scale linear mountain belts (see section 3) using the half-width

2

of the range and the mean outlet spacing. He found that the ratio between these two values (drainage spacing ratio, R) was extremely consistent (between 1.91 and 2.23) for the 11 orogens studied, irrespective of age and climate. His method has since been applied to smaller, younger fault blocks (Talling *et al.*, 1997; Purdie & Brook, 2006), where outlet spacing was again found to be regular.

Drainage spacing has not previously been investigated at mountain range fronts affected by strike-slip faulting, where it may be affected by the fault movement and resultant complex topography. This study investigates the relationship between river systems, faulting and topography for the Kuh Banan Fault in eastern Iran (Fig. 1), which is an active strike-slip fault with relief across it, caused by a component of thrusting. Firstly, offsets at varying scales are documented, and possible controls affecting the size of offsets are considered. Secondly, drainage spacing on the Kuh Banan Fault is investigated, and properties influencing it are discussed.

2. Tectonic Setting

Active deformation in Iran is related to the Arabia-Eurasia collision, which causes ~25mm/yr of roughly north-south convergence at longitude ~56°E (Vernant *et al.*, 2004). The deformation occurs largely within a compact area delimited by the political borders of Iran (Walker *et al.* 2010), and is mostly accommodated in the compressional zones of the Zagros Mountains in the south, and the Alborz and Kopeh Dagh mountains in northern Iran (Fig. 1a). GPS studies suggest that ~10 mm/yr of convergence is taken up in the central Zagros (Tatar *et al.*, 2002).

The remaining shortening is accounted for by the northward movement of central Iran with respect to Afghanistan (Fig. 1a) at 16±2 mm/yr (Vernant *et al.*, 2004). This right-lateral shear is taken up on N-S to NW-SE strike-slip faults in eastern Iran (Meyer & Le Dortz, 2007) by both right-lateral slip and anticlockwise rotation (Walker & Jackson, 2004; Allen *et*

al., 2011), and on left-lateral faults north of 34°N trending between E-W and N70°E, which are thought to rotate in a clockwise direction (Jackson & McKenzie, 1984). The Arabia-Eurasia collision is thought to have undergone a significant reorganisation at 5±2 Ma (Allen *et al.*, 2004; Copley & Jackson, 2006), based on changes in deformation and sedimentation (e.g. Axen *et al.*, 2001; Westaway, 1994) and the time needed to extrapolate active slip rates to achieve the total fault slip (Allen *et al.*, 2004). Meyer & Le Dortz (2007) propose an earlier date of 8-22 Ma. These active faults in places postdate earlier patterns of deformation, some of which is related to the construction of the Turkish-Iranian plateau (Morley *et al.,* 2009; Mouthereau, 2011).

The Kuh Banan Fault is a ~180km long right-lateral strike-slip fault located east of the city of Zarand (Fig. 1b). It has a NNW-SSE trend, roughly parallel to other strike-slip faults in the region (Behabad, Jorjafk and Rafsanjan) (Allen *et al.*, 2011). Adjacent to the fault there is ~1 km of topography, which switches from the west to the east side of the fault trace towards its northern end, suggesting a reversal of fault plane dip. This topography indicates that there is a thrust component to the fault movement; however, the fault plane solution of the Bob Tangol earthquake in 1977 (Berberian *et al.*, 1979) indicates mainly strike-slip motion with only a small amount of thrusting. The Kuh Banan Fault therefore appears to have changed from being a thrust or oblique thrust fault to the dominantly strike-slip fault seen today (Walker *et al.*, 2010).

At its southern end, the Kuh Banan Fault is simple and linear, but to the north it becomes fragmented into several strands (Mahdavi, 1996). There are two possible pull-apart basins located at bends in the fault trace (Allen *et al.*, 2011) (Fig. 1b). Total fault offset is uncertain, although Berberian (2005) determined a minimum offset of 5 km based on the displacement of Cambrian and Jurassic strata. Since the length of a pull-apart basin may serve as a minimum estimate for total offset along a strike-slip fault (Mann *et al.* 1983), the length

of the southern pull-apart suggests that the minimum offset is ~7 km. The slip-rate of the Kuh Banan Fault is estimated at 1-2 mm/yr. This is based on stream offsets assumed to have formed since ~12±2 ka, when regional climate change resulted in widespread incision, and the fact that the fault does not perturb the regional GPS velocity field (Allen *et al*., 2011; Meyer & Le Dortz, 2007).

The Kuh Banan Fault is seismically active (Berberian *et al.*, 1979; Talebian *et al.*, 2006). Numerous earthquakes have been recorded (Fig. 1b), including the M_s 5.8 Bob-Tangol earthquake at 30.9ºN 56.6ºE on 19th December 1977 (Berberian *et al.*, 1979) and other large events in 1933 and 1978 on the northern section of the fault. Earthquakes have also occurred on nearby faults, including the Dahuiyeh thrust which ruptured in 2005 (Talebian *et al.*, 2006) and the Behabad fault (Ambraseys and Melville, 1982).

3. Methodology and data

High-resolution satellite imagery (acquired from Quickbird, SPOT and GeoEye-1 satellites and viewed in Google Earth) and Shuttle Radar Topography Mission (SRTM) digital topographic data were used in this study (Rodriguez *et al.*, 2005; Jarvis *et al.*, 2008). SRTM data have a specified vertical absolute accuracy of ≤16 m (Rodriguez *et al.* 2005). Gorokhovich and Voustianiouk (2006) found it ranged from 7.58±0.60 m to 4.07±0.47 m in two local case studies. Specific vertical relative accuracy is quoted as ≤10 m (Rodriguez *et al.* 2005).

Satellite images were used to measure the offset (parallel to the fault trace) and the drainage length (taken to be the distance from the point where the river crosses the fault trace to the source of the most distant tributary) of rivers along the Kuh Banan Fault. In order to accurately measure the offset, the upstream and downstream course of each river was projected onto the fault trace (Fu e*t al*., 2005) (Fig. 2a). Offsets in the opposite sense to fault movement can occur via stream capture (Fu *et al.*, 2005; Huang, 1993) (Fig. 2b), so to avoid

bias in the measurements apparent left-lateral offsets were also measured. Since the fault is right-lateral, however, these left-lateral offsets were not considered for the bulk of the study. The gradients of the largest rivers were measured from SRTM data in order to see how gradient varies across the fault.

The method devised by Hovius (1996) was then applied to rivers along the Kuh Banan Fault (Fig. 3). Due to the highly variable topography along the Kuh Banan Fault there is no simple, single main drainage divide, so the mountain range was divided into ten separate ridges (Fig. 1b) which formed local drainage divides. Each ridge was treated as a separate mountain range for the purpose of drainage spacing calculation. There are no wind or water gaps within these ridges. The outlet spacing (s) of adjacent catchments with trunk streams originating at the main drainage divide was measured, as was the ridge half-width (w), defined as the distance between the mountain front and the drainage divide (Fig. 4a). The means of these values were used to calculate the spacing ratio (R) for each ridge using the equation $R = W/S$, where W and S are the mean values of w and s. Spacing ratios for individual catchments were also determined and their mean (R') calculated for each ridge. Since R' is greatly affected by outliers and may not therefore be representative of the ridge as a whole, the value of R was used to characterise the drainage spacing of each ridge.

The ridges and folds used were often nonlinear, so the local half-widths (w_{local}) of individual catchments were averaged to get a more accurate measurement. Outlet spacing s was measured parallel to the mountain front and w was measured perpendicular to it (Fig. 4a). All rivers that originated within $0.1w_{local}$ of the main divide (henceforth referred to as "main rivers") were included, provided they did not merge with another main river further than $0.02w_{local}$ upstream of the mountain front, as specified by Hovius (1996). The standard deviations (σ_s and $\sigma_{r)}$ of S and R', respectively, were calculated. It was found that σ_s tends to

6

increase with the magnitude of S, so the ratio between S and σ_s ($\sigma\%$) was determined in order to better quantify the regularity of outlet spacing.

The sinuosity of each ridge and fold was calculated using the method devised by Keller & Pinter (1996) to see if there is a correlation between sinuosity and drainage parameters. Any such correlation would have to be accounted for in making further interpretations of the drainage data. First the total length of the mountain front between two points was measured and then this length was divided by the distance between those two points in a straight line. This process was then repeated for the ridge crest (Fig. 4b).

4. Results

4.1 River offsets

187 offset rivers were measured along the Kuh Banan Fault (see Appendix 1): 153 right-lateral (Figs. 5a-f) and 34 left-lateral (Figs. 5g & 6a). Right-lateral offsets range from 4 to 3478 m with a mean of 170 m. 104 of the rivers have offsets smaller than 100 m, and only 12 have offsets greater than 500 m. The largest (>1 km) offsets are typically located behind shutter ridges (i.e. ridges which have been displaced along the fault) (Fig. 5e). Left-lateral offsets are in general much smaller (Fig. 6a) ranging from 4 to 290 m, except for one extremely large offset of 2272 m (which appears to have been deflected by a shutter ridge). Several of the main rivers on ridges 1, 2, 3, 5 and 9 (see section 3; Fig. 3) have been offset (see appendix 2). The mean offset varies from 45m to 1097 m (Table 1). There is a positive correlation between offset (D) and drainage length (L). The line of best fit has an r^2 value of 0.79 and an equation of $L = 5.24D + 279$ (Fig. 6b). There are several clusters of offset length, at 0-50 m, 50-100 m, 100-200 m, 200-300 m, 350-500 m, and >500 m (Fig. 6c).

Fig. 6d shows that the gradient of rivers tends to decrease where the river is offset. This is due to the dominantly strike-slip movement of the fault. Each end of the offset is moved only laterally, not vertically, so that the elevations of the two points do not change

7

significantly with fault slip. Since the horizontal distance between them increases but the vertical distance remains the same, the gradient of the offset must decrease.

4.2 Drainage spacing

There is significant variability in half-width and spacing both between ridges and within each ridge (Table 1; Fig. 3; see appendix 2). W varies between 364 m and 6122 m; within a single ridge w can vary by up to 4 km. S ranges from 173 m to 5652 m. Spacing is highly irregular in six of the ridges ($\sigma\%$ is between 0.59 and 0.9).

Variation in spacing ratio R is also large, varying between 1.1 and 3.1. The mean ratio is 1.8, smaller than the value of 2.1 determined by Hovius (1996) but within his range of values. Spacing ratio also varies significantly within ridges 3, 4, 5 and 7 (σ_r is between 1.45 and 5.73), but is more consistent within the others (Table 1). There is a clear correlation between the half-width of the ridge and the outlet spacing (Fig. 7a; see section 4.2). A relationship also exists between the spacing of the main rivers on several ridges and their mean offset (Fig. 7b). The equation of the regression line is $S = 3.17D + 193$, and the r^2 value is 0.91, showing that the mean offset is ~3 times smaller than the mean spacing. KB 1 was not included in Fig. 7b because it has only one offset.

4.3 Sinuosity

Sinuosity is variable along the Kuh Banan Fault. Mountain fronts are typically less sinuous than crests. No correlation exists between sinuosity (of either mountain fronts or crests) and either outlet spacing regularity ($\sigma\%$) or spacing ratio R (Figs. 7d-e).

4.4 Uncertainty

Given that the tools and imagery used for the measurements outlined in section 3 are accurate to within 0.5%, uncertainty in these results arises almost exclusively from human inaccuracy and is therefore extremely difficult to quantify. The most inaccurate measurements

are the ridge half-widths, since the precise location of the crest and mountain front is often unclear, and the drainage lengths, because it can be difficult to determine the location of the source of a river (especially for larger catchments). Offset and outlet spacing measurements are also subject to error, but repeated measurements show that this error is likely to be less than ~5%. This could be reduced by measuring each offset and outlet spacing three or more times, but limited time made this approach unfeasible.

Another potential source of error is the fact that w was measured horizontally across each ridge in this study, whereas Hovius (1996) measured the diagonal widths of his mountain ranges. However, the difference between horizontal and diagonal widths in this area is small (<5%) and hence the results of the two studies can still be directly compared. In summary, uncertainty is not formally quantified in this study. It is expected that total error will be on the order of a few percent and therefore is not significant.

5. Discussion

5.1 River offsets

The most striking aspect of the Kuh Banan Fault is the number of river offsets that are present along its length (see Appendix 1), as previously reported by Berberian *et al.,* (1979). A brief examination shows that other strike-slip faults in the region do not preserve nearly as many, despite having similar number of drainages. The reason for this is not known for certain, but may be related to the rates of uplift and lateral movement on the Kuh Banan Fault. Both of these are required in order to create and preserve offsets, since a fault with only vertical movement would create topography but no offsets; whereas a purely strike-slip fault creates no topography, allowing rivers to meander freely across the fault trace and thus preserving no offsets. The Kuh Banan Fault is thought to have a greater slip rate than the similarly-uplifted Jorjafk fault (estimated slip rate <1 mm/yr); it also has higher topography (suggesting a greater rate of uplift) than the nearby Behabad fault, which slips at a similar rate

9

(Fig. 1b) (Allen *et al.*, 2011). It is therefore probable that the movement of the Kuh Banan Fault is simply better suited to preserving river offsets than that of nearby faults, by virtue of its component of dip slip motion. It is possible that thrust motion and surface uplift in the region slightly preceded strike-slip deformation (Walker *et al.*, 2010), implying that at least the larger scale drainage patterns also pre-date the strike-slip.

The observation that uplift is required for offset preservation explains the distribution of offsets seen along the Kuh Banan Fault. Most offsets are found on the uplifted southern section of the fault, with very few being observed towards the northern end which is located within an alluvial plain (Fig. 1b).

The key observation highlighted by Fig. 6b is a lack of river offsets along the Kuh Banan Fault comparable to the bedrock offset. The presumed age of the fault (~5 Ma; Allen *et al.*, 2004) combined with the estimated slip rate of 1-2 mm/yr (Allen *et al.*, 2011) suggests that there should be offset on the order of 5-10 km. Even if slip rate was lower in the past, or the fault is younger than 5 Myr, the minimum total displacement of ~5-7 km determined by Berberian (2005) and this study (see section 2) is greater than the maximum river offset of ~3.5 km.

One possible explanation for this discrepancy is climate change, resulting in changes in base-level. If base-level rose sufficiently to encroach on the margin of the topography adjacent to the Kuh Banan Fault, the rivers would no longer flow along the fault but straight into the newly-formed lake. This would obliterate all offset channels so that when base level fell and the lake drained away the rivers would flow straight across the fault trace (Fig. 8a). Present-day base level is in the region of Zarand (Fig. 1b), at an elevation of ~1650 m. By contrast the elevation of the mountain front is ~2000 m, meaning that a base-level rise of ~350 m would be required. This is unfeasible, as there are numerous lower-elevation spill-

points around the edges of the regional drainage basin which would prevent the rising water reaching the Kuh Banan mountain front.

A widespread fall in base-level, on the other hand, would result in increased river incision, which acts to straighten stream courses (Huang, 1993). However, this would not significantly decrease offsets, especially for larger rivers and displacements, and cannot therefore account for the difference between the 5-7 km geological offset and the 3.5 km river offset.

An extremely arid climate would cause the rivers to completely dry up. If they were dry for long enough continued fault movement would further offset the valleys on either side of the fault. Without river flow and incision the near-zero gradient (Fig. 6d) along the fault could conceivably break the connection between the valleys. When the rivers resumed flow they would have to find a new downstream course, invariably resulting in a smaller apparent offset than had previously existed (Fig. 8b). The valleys would need to be separated by several hundred metres to break the connection, however, and with a slip rate of 2 mm/yr the rivers would have to be dry for >100 ka. It is highly unlikely that the climate of eastern Iran was sufficiently arid for such a long period of time: Walker and Fattahi (2011) demonstrated the late Pleistocene/Holocene variability of east Iranian climate, on timescales far shorter than 100 ka.

A more likely explanation is stream capture (Fig. 2b; see section 3). This is a common process on the Kuh Banan Fault as shown by the occurrence of left-lateral offsets (Fig. 5g). In some cases it is possible to identify the old (right-lateral) course of a river that has recently been captured (Fig. 5g), showing that this is a viable mechanism for resetting the apparent offset of a stream (as suggested by Replumaz *et al.*, 2001). While these instances are rare and mostly confined to smaller streams, the same process will also occur with larger rivers. Once the river was captured and the offset reset, further fault slip would result in a new, smaller

right-lateral offset (Fig. 2b). Streams on the alluvial plain may also be capable of capture through backwards erosion of their headwaters. Stream capture is likely to be promoted by the shallow river gradient along the fault trace, as this makes the original course more difficult to maintain. This process could account for the gap between the largest (~3.5 km) offset and the next largest (~1.6 km): the larger occurs on an unusual section of the fault, where there are no rivers nearby that could capture it (Fig. 5b), while the other rivers are surrounded by streams.

Finally, a river may alter its own course in order to take advantage of an easier pathway, thereby reducing its apparent offset. This is possible if the gradient along the fault becomes low enough to cause spontaneous rerouting of the river, but may not occur under normal conditions since incision and the thrust component to the fault's movement help maintain an above-zero gradient. If, however, the region experienced exceptional levels of rainfall which caused flooding, a river may burst its banks in a manner analogous to levee breach, and erode a new pathway onto the alluvial plain (Fig. 8c). This new route would have a steeper gradient than the offset section of the river, so that when water levels fell the stream would make use of the new channel and abandon the old one. This process is instantaneous in geological terms, and hence is difficult to identify unless it is being observed at the time of breach. It is not possible therefore to determine whether this has occurred on the Kuh Banan Fault. The shallow gradient along the fault trace may also make it more likely for a river to significantly alter its course in response to a blockage, such as a landslide.

The common coexistence of shutter ridges and large (>1 km) displacements (see section 4), suggests that the ridges aid the formation of large offsets, by protecting against stream capture. It is unlikely that these ridges have artificially enlarged the offset as rivers are clearly displaced by the fault before encountering the ridge (Fig. 5e). This protection is twofold: firstly, streams on the alluvial plain would have to erode through the ridge; secondly, the topography would deflect the course of any other offset streams that might be capable of

capture (Fig. 8d). The few large offsets not protected by a shutter ridge are invariably deeply incised into the bedrock, which provides similar (and longer-lasting) protection from stream capture.

These effects would persist only for as long as the shutter ridge was located opposite the river. As soon as it is displaced enough to leave part of the river open to the alluvial plain, the river is again vulnerable to capture, which is why offsets larger than a few kilometres are not produced by shutter ridges. This may explain the gap between the two largest offsets, because the ~3.5 km offset is protected by a ridge much longer than any others on the Kuh Banan Fault (Fig. 5a).

Shutter ridges may also facilitate course adjustments of rivers in response to the shallow gradient along the fault. Once the shutter ridge is displaced enough to leave the upstream section of the river open to the alluvial plain, a much easier pathway for the river would exist by flowing past the end of the shutter ridge rather than all the way around it (Fig. 8d).

The relationship observed in Fig. 6b, where drainage length has a positive correlation with offset, would be expected even if stream capture or other rerouting processes did not operate, because drainage length and offset both increase with the age of a river. Many of the offsets are likely to have been modified, however, so it interesting that the correlation between drainage length and offset exists. This indicates that there is a relationship between the size of a river and how often it is captured, assuming stream capture is the dominant process limiting offset size. Smaller rivers are never offset by large amounts (and are presumably captured before large offsets can form) while the larger rivers can accumulate a larger offset before they are captured. This could be because drainage spacing controls river capture (as postulated by Huang, 1993) and, ultimately, offset. A river can never be offset by a greater amount than the distance to the next stream capable of capture, since capture will

occur and the offset will be reset as soon as the two rivers are close enough (Fig. 2b). Smaller rivers occur close together, and therefore capture occurs before the offset can reach more than a few tens or hundreds of metres; whereas the larger rivers are much more widely spaced (and presumably can only be captured by rivers of a comparable size) allowing the offsets to grow. Capture occurring at different scales may account for the clustering seen in Fig. 6c.

It is interesting that it does not seem to matter whether the rivers are perennial or not; there is no clear jump in the ratio data which might correspond to a switch from ephemeral or intermittent to perennial drainage (Fig. 6).

5.2 Drainage spacing and sinuosity

The high values of σ_r (Table 1) show that the spacing ratio of individual drainage basins is highly variable. Generally, however, there is a predominance of values of around 2 – high σ_r values tend to be due to a small number of basins with anomalously high or low ratios. This suggests that the relationship between *W* and *S* applies to individual drainage basins as well as entire drainage networks.

There is no clear systematic variation in *R* with location on the Kuh Banan Fault, although both the highest and lowest values are found at the ends of the fault trace. In general lower *R*-values are found on the northern half of the fault (Fig. 1b; Table 1). The highest value of *R* (3.2) is found on ridge KB 1 at the southern end of the fault, where the topography is dominated by a pair of steeply-plunging folds (Fig. 9a). Several stratigraphic units within these folds are resistant to erosion and form distinct topographic ridges. These have influenced the courses of the main rivers resulting in long and narrow drainage basins. The structure of the mountain range in this location has therefore produced a closer spacing than would have existed otherwise.

Topography seems to have exerted a similar control on ridge KB 10 with the lowest R-value of 1.1. In this case however there are several topographically high blocks that have clearly deflected the main rivers (Figs. 9b-c). These blocks are deeply incised by smaller streams and are therefore unlikely to be caused by a resistant lithology, but may be a result of differential uplift within the ridge. The deflection results in very broad drainage basins, and hence a wider-than-typical outlet spacing. A similar process appears to have occurred on other ridges with anomalously low (<1.5) spacing ratios.

Talling *et al.* (1997) determined that S was irregular for fault blocks with sinuous mountain fronts. The results of this study however suggest that this is not the case (Figs. 7d-e), and that sinuosity of either mountain fronts or ridge crests has no effect on drainage spacing.

Hovius (1996) found a mean spacing ratio of 2.1, larger than that determined for the Kuh Banan ridges in this study (1.8). This suggests that drainages along the Kuh Banan Fault tend to be more widely spaced than those in the larger mountain belts studied by Hovius (1996). The difference between the mean R value for the Kuh Banan Fault and the larger mountain belts is intriguing, especially given the general consistency within Hovius's (1996) results. This is unlikely to be due to differences in ridge half-width, even though the mountain belts are $1 - 2$ orders of magnitude larger than the Kuh Banan ridges (Fig. 7c), as the smallest ridge measured for Kuh Banan ($W = 364$ m) has a ratio of 2.1. A more likely possibility is that variable topography (Fig. 9) has resulted in a lower spacing ratio. There is no evidence to suggest that the strike-slip movement of the Kuh Banan Fault has had any effect on the spacing ratio.

Talling *et al.* (1997) investigated drainage spacing for fault blocks in the United States and determined an average ratio of 2.5, with individual blocks varying between 1.4 and 4.1, a far greater range than that of Hovius (1996). They concluded that this was due to local factors

such as uplift rate, precipitation and lithology, and noted that it is enigmatic why such factors do not carry through to the larger mountain ranges studied by Hovius (1996), or even the Kuh Banan Fault described in this study. The overall aridity of eastern Iran means that variation in precipitation patterns cannot be an important control and it has already been determined that lithology has no effect on spacing ratio, but variable uplift may have caused the structural complexity resulting in low spacing ratios on the Kuh Banan Fault.

Purdie and Brook (2006) looked at drainage spacing on the Ruahine Range in New Zealand. They found an extremely low R value of 1.31, and interpreted this as being due to fault splays which resulted in widening of drainage basins. This is not the case for the Kuh Banan Fault, but also suggests that structural complexity can have a major effect on drainage spacing on small scales.

5.3 Relationship between drainage spacing and offset

Given the hypothesis that drainage spacing controls how often stream capture occurs (see section 5.1), there should be a relationship between the mean observed offset of main rivers on the Kuh Banan Fault and the outlet spacing of those rivers (assuming that only streams of similar or larger size are capable of capturing each other). We would expect the mean offset to be close to, but never more than, the mean outlet spacing. Table 1 clearly shows that not only is the mean offset consistently much smaller than the mean outlet spacing, but that the maximum offset is also much smaller. The offset on ridge 7 is much more comparable to the mean spacing than for other ridges. It is, however, based on restoration of a beheaded alluvial fan (Fig. 5f) and hence is not affected by stream capture. At first sight, this suggests that outlet spacing cannot control the maximum offset observed on the fault. However, the consistent relationship shown in Fig. 7b, where the mean spacing is ~3 times larger than the mean offset for all ridges, strongly indicates that offset size is related to drainage spacing by this scale-independent ratio, as shown schematically in Fig. 10.

16

6. Conclusions

Right-lateral movement of the Kuh Banan Fault has resulted in the formation of numerous river offsets (Fig. 6). The slip rate and uplift of the Kuh Banan Fault allow good preservation of offsets along much of the fault trace (Fig. 5). Abandoned channels downstream of the fault trace are, however, easily eradicated through alluvial fan deposition, making it impossible to perform offset reconstructions to determine the fault's total displacement.

Although the total displacement of the fault is uncertain, minimum values of 5-7 km have been determined from geological offsets (Berberian, 2005) and the length of pull-apart basins (this study). The maximum observed river offset of ~3.5 km is therefore lower than the total offset. Several hypotheses have been proposed to explain this relationship, including climate change (resulting in base level rise, river incision or complete aridification of the region, depending on the climatic shift), stream capture, and gradient-related adjustments of stream profile (Fig. 8). The various climate-change hypotheses are rejected on the basis of observational and theoretical evidence: spill points at the edges of the regional drainage basin would prevent base level from reaching the Kuh Banan Fault; river incision would not substantially reduce large offsets; and the region would have to be completely dry for an unfeasibly long period of time in order to separate the upstream and downstream channels and cause changes in stream course. Adjustments of streams related to the shallow gradient of the fault may be effective under special circumstances but are unlikely to occur normally. Stream capture is therefore the favoured mechanism for reducing the size of apparent offsets. Stream capture appears to be controlled by drainage spacing such that smaller, closely-spaced rivers are only offset by <100 m before being captured, while larger, more widely-spaced rivers can accumulate much larger offsets. Shutter ridges encourage formation of large offsets through protection from stream capture and prevention of autonomic river adjustments.

17

Drainage spacing ratios of the Kuh Banan Fault are highly variable (Fig. 7) with a mean (1.8) significantly smaller than that determined by Hovius (1996) for larger ranges (2.1). This is attributed to structural complexity and resultant topographic variation deflecting rivers and affecting drainage basin shapes on smaller scales. The lateral movement of the Kuh Banan Fault does not appear to significantly affect the spacing or geometry of drainage basins.

While drainage spacing seems to control the mean offset of rivers along the Kuh Banan Fault the relationship is not simple. Main rivers can be captured by smaller streams (not originating at the main drainage divide) such that the size of their offset never approaches their spacing (mean spacing is typically 3 times larger than the mean offset; Fig. 10).

Although both river offsets and drainage spacing have been investigated previously, this study is the first to have combined the two to determine the effect that spacing has on offset. Further investigation utilising knowledge of river dynamics is needed to establish the exact relationship.

Acknowledgements

References

Allen, M. B., Kheirkhah, M., Emami, M. H., Jones, S. J., 2011. Right-lateral shear across Iran and kinematic change in the Arabia-Eurasia collision zone. Geophys. J. Int., 184, 555-574.

Allen, M., Jackson, J., Walker, R., 2004. Late Cenozoic reorganization of the Arabia-Eurasia collision and the comparison of short-term and long-term deformation rates. Tectonics, 23, TC2008, doi: 10.1029/2003TC001530.

Ambraseys, N. N., Melville, C. P., 1982. A history of Persian earthquakes. Cambridge University Press, New York, pp. 164-166.

Axen, G. J., Lam, P. S., Grove, M., Stockli, D. F., Hassanzadeh, J., 2001. Exhumation of the west-central Alborz Mountains, Iran, Caspian subsidence, and collision-related tectonics. Geology, 29, 559-562.

Berberian, M., Asudeh, I., Arshadi, S., 1979. Surface rupture and mechanism of the Bob-Tangol (Southeastern Iran) earthquake of 19 December 1977. Earth Planet. Sci. Lett., 42, 456-462.

Berberian, M., 2005. The 2003 Bam Urban Earthquake: A Predictable Seismotectonic Pattern Along the Western Margin on the Rigid Lut Block, Southeast Iran. Earthq. Spectra, 21 (S1), S35-S99.

Copley, A., Jackson, J., 2006. Active tectonics of the Turkish-Iranian Plateau. Tectonics, 25, TC6006, doi: 10.1029/2005TC001906.

Cowgill, E., 2007. Impact of riser reconstructions on estimation of secular variation in rates of strike-slip faulting: Revisiting the Cherchen River site along the Altyn Tagh Fault, NW China. Earth Planet. Sci. Lett., 254, 239-255.

Cowgill, E., Gold, R.D., Chen, X.H., Wang, X.F., Arrowsmith, J.R., Southon, J., 2009. Low Quaternary slip rate reconciles geodetic and geologic rates along the Altyn Tagh fault, northwestern Tibet. Geology, 37, 647-650.

Fu, B., Awata, Y., 2007. Displacement and timing of left-lateral faulting in the Kunlun Fault Zone, northern Tibet, inferred from geologic and geomorphic features. J. Asian Earth Sci., 29, 253-265.

Fu. B., Awata, Y., Du, J., He, W., 2005. Late Quaternary systematic stream offsets caused by repeated large seismic events along the Kunlun fault, northern Tibet. Geomorphology, 71, 278-292.

Gorokhovich, Y., Voustianiouk, A., 2006. Accuracy assessment of the processed SRTM-based elevation data by CGIAR using field data from USA and Thailand and its relation to the terrain characteristics, Remote Sens. Environ., 104, 409-415.

Hovius, N., 1996. Regular spacing of drainage outlets from linear mountain belts. Basin Res., 8, 29-44.

Huang, W., 1993. Morphologic patterns of stream channels on the active Yishi Fault, southern Shandong Province, Eastern China: implications for repeated great earthquakes in the Holocene. Tectonophysics, 219, 283-304.

Jackson, J., Norris, R., Youngson, J., 1996. The structural evolution of active fault and fold systems in central Otago, New Zealand: evidence revealed by drainage patterns. J. Struct. Geol., 18, 217-234.

Jackson, J., McKenzie, D., 1984. Active tectonics of the Alpine-Himalayan belt between Turkey and Pakistan. Geophys. J. Roy. Astr. Soc., 77, 185-264.

Jarvis, A., Reuter, H.I., Nelson, A., Guevara, E., 2008. Hole-filled SRTM for the globe Version 4, available from the CGIAR-CSI SRTM 90m Database (http://srtm.csi.cgiar.org).

Keller, E. A., Pinter, N., 1996. Active Tectonics: Earthquakes, Uplift, and Landscape. Prentice Hall, New York, pp. 138.

Mahdavi, M. A., 1996. Geological Quadrangle map of Iran, 1:250,000 scale, sheet NH 40.2 (Ravar), Geological Survey of Iran.

Mann, P., Hempton, M. R., Bradley, D. C., Burke, K., 1983. Development of pull-apart basins. J. Geol., 91, 529-554.

Meyer, B., Le Dortz, K., 2007. Strike-slip kinematics in Central and Eastern Iran: Estimating fault slip-rates averaged over the Holocene. Tectonics, 26, TC5009, doi: 10.1029/2006TC002073.

Morley, C.K., Kongwung, B., Julapour, A.A., Abdolghafourian, M., Hajian, M., Waples, D., Warren, J., Otterdoom, H., Srisuriyon, K., Kazemi, H., 2009. Structural development of a major late Cenozoic basin and transpressional belt in central Iran: The Central Basin in the Qom-Saveh area. Geosphere, 5, 325-362.

Mouthereau, F., 2011. Timing of uplift in the Zagros belt/Iranian plateau and accommodation of late Cenozoic Arabia–Eurasia convergence. Geol. Mag., 148, 726-738.

Purdie, H., Brook, M., 2006. Drainage spacing regularity on a fault-block: A case study from the eastern Ruahine Range. New Zeal. Geogr., 62, 97-104.

Replumaz, A., Lacassin, R., Tapponnier, P., Leloup, P. H., 2001. Large river offsets and Plio-Quaternary dextral slip rate on the Red River fault (Yunnan, China). J. Geophys. Res., 106 (B10), 819-836.

Rodriguez, E., Morris, C.S., Belz, J.E., Chapin, E.C., Martin, J.M., Daffer, W., Hensley, S., 2005. An assessment of the SRTM topographic products, Jet Propulsion Laboratory, Pasadena, California, Technical Report D-31639, 1-143.

Sylvester, A. G., 1988. Strike-slip faults. Geol. Soc. Am. Bull., 100, 1666-1703.

Talebian, M., Biggs, J., Bolourchi, M., Copley, A., Ghassemi, A., Ghorashi, M., Hollingsworth, J., Jackson, J., Nissen, E., Oveisi, B., Parsons, B., Priestley, K., Saiidi, A., 2006. The Dahuiyeh (Zarand) earthquake of 2005 February 22 in central Iran: reactivation of an intramountain reverse fault. Geophys. J. Int., 164, 137-148.

Talebian, M., Jackson, J., 2002. Offset of the Main Recent Fault of NW Iran and implications for the late Cenozoic tectonics of the Arabia-Eurasia collision zone. Geophys. J. Int., 150, 422-439.

Talling, P. J., Stewart, M. D., Stark, C. P., Gupta, S., Vincent, S. J., 1997. Regular spacing of drainage outlets from linear fault blocks. Basin Res., 9, 275-302.

Tatar, M., Hatzfeld, D., Martinod, J., Walpersdorf, A., Ghafori-Ashtiany, M., Chéry, J., 2002. The present-day deformation of the central Zagros from GPS measurements. Geophys. Res. Lett., 29 (19), 1927, doi: 10.1029/2002GL015427.

Vernant, P., Nilforoushan, F., Hatzfeld, D., Abbassi, M. R., Vigny, C., Masson, F., Nankali, H., Martinod, J., Ashtiani, A., Bayer, R., Tavakoli, F., Chéry, J., 2004. Present-day crustal deformation and plate kinematics in the Middle East constrained by GPS measurements in Iran and northern Oman. Geophys. J. Int., 157, 381-398.

Walker, R., Jackson, J., 2004. Active tectonics and late Cenozoic strain distribution in central and eastern Iran. Tectonics, 23, TC5010, doi: 10.1029/2003TC001529.

Walker, R. T., Talebian, M., Saiffori, S., Sloan, R. A., Rasheedi, A., MacBean, N., Ghassemi, A., 2010. Active faulting, earthquakes and restraining bend development near Kerman city in southeastern Iran. J. Struct. Geol., 32, 1046-1060.

Walker, R.T., Fattahi, M., 2011. A framework of Holocene and Late Pleistocene environmental change in eastern Iran inferred from the dating of periods of alluvial fan abandonment, river terracing, and lake deposition, Quat. Sci. Rev., 30, 1256-1271.

Westaway, R., 1994. Present-day kinematics of the Middle East and eastern Mediterranean. J. Geophys. Res., 99 (B6), 12071-12090.

Figure Captions

Figure 1. Location maps. (a) Location of the study area (satellite image ©2011 Google; LeadDog Consulting; Europa Technologies). Black lines are the national borders of Iran. Arrow shows the movement of Iran relative to Afghanistan. (b) Map showing major faults of the Kuh Banan region overlain on an SRTM image (Allen *et al.*, 2011). Numbers refer to the locations of ridges used for drainage spacing (Fig. 3 & Table 1). Sub-parallel right-lateral strike-slip faults are dominant and associated with significant topography due to a component of thrusting. Two pull-apart basins are located at bends in the Kuh Banan Fault, located between ridges KB5 and KB6 and KB9 and KB10. Earthquake focal mechanisms from Talebian *et al.* (2006) for the 1977 and 2005 events, and the Harvard catalogue (http://www.globalcmt.org; records filtered for >70% double-couple solutions) for the 2007 event. Other epicentres (M_w>4.5), given by white circles, are from the National Earthquake Information Center (NEIC) catalogue (http://earthquake.usgs.gov/earthquakes/) and Ambraseys and Melville (1982).

Figure 2. Form of river channels across a right-lateral strike-slip fault. (a) Measurement of stream offset across the fault trace. (b) Schematic diagram showing stream capture and the resulting left-lateral (opposite sense to the fault movement) offset (t=1). Further fault movement causes evolution of the left-lateral offset back into a smaller right-lateral offset (t=3).

Figure 3. Drainage basins along ridges used in drainage spacing calculations. "KB #" refers to ridges on the Kuh Banan Fault. Redrawn from satellite imagery. Scale bars represent a horizontal distance of 1 km and arrows indicate northward direction. Location numbers refer to those given in Table 1 and Figs. 1b-c.

Figure 4. Drainage spacing and sinuosity methodologies. (a) Schematic view of drainage basins on a ridge, showing the parameters used to calculate drainage spacing (after Hovius,

1996). Local half-width (w_1 and w_2) of each adjacent river was measured from the mountain front to the ridge crest, perpendicular to the mountain front, and averaged to give the ridge half-width (w). Outlet spacing (s) between adjacent drainage outlets was measured in a straight line parallel to the mountain front. (b) Schematic of a mountain front, showing the parameters used to calculate sinuosity. The total length of the mountain front, shown in bold, is divided by the length in a straight line to give the sinuosity.

Figure 5. SRTM and satellite images (©2011 Google; GeoEye; DigitalGlobe; Cnes/Spot Image) of river offsets along the Kuh Banan Fault. White arrows highlight the fault trace. (a) The largest offset is ~3.5 km long. (b) Smaller offset clearly showing the position of the Kuh Banan Fault. (c) The smallest offsets are just a few metres. These streams are offset by 14 m and 7 m. (d) Four streams with ~70m offset. Offset reconstruction matches the channels A, B, C and D with the valleys A', B', C' and D'. (e) 3D view of an offset behind a shutter ridge. (f) Beheaded alluvial fan (hatched area). The dotted line shows the river likely to have formed the fan.   (g) Left-laterally offset stream. Stream *A* has recently been captured and now flows into stream *B*, leaving a dry gulley, *C* (dashed white line), where the original stream course lay.

Figure 6. Graphical representation of offsets on the Kuh Banan Fault. (a) Plot comparing the number and sizes of right lateral vs. left lateral offsets. Right-lateral offsets dominate. (b) Plot showing the correlation between drainage length and offset for right-lateral offsets.
(c) Enlarged section of (b), showing detail of offsets smaller than 500m. Clusters occur at 0-50 m, 50-100 m, 100-200 m, 200-300 m and 350-500 m. (d) Gradients of large rivers along the Kuh Banan Fault, derived from SRTM data. The gradient decreases as the rivers cross the fault trace.

Figure 7. Graphs of drainage spacing and sinuosity. (a) Plot of ridge half-width (*W*) against outlet spacing (*S*). (b) Plot of the mean spacing of main rivers against their mean offset. (c)

Points in (a) superimposed on the plot from Hovius (1996). Regression line and red points are from Hovius (1996). (d) Sinuosity of ridges compared to outlet spacing regularity. (e) Sinuosity of ridges compared to spacing ratio.

Figure 8. Diagrams illustrating possible mechanisms for reducing the apparent stream offset. Dashed lines show abandoned valleys. See text for details. (a) Rising base level creates a lake with its margin along the Kuh Banan Fault (t=1), eradicating offsets (t=2). (b) Aridification of the region causes the stream to dry up (t=1). Continued fault movement breaks the connection between the dry valleys on either side of the fault (t=2), so that when the stream resumes flow it must find a new route across the fault (t=3). (c) Flooding of a river results in erosion of a new channel (t=1). When river levels fall back to normal this pathway is utilized because it has a steeper gradient than the offset (t=2). (d) Shutter ridge (hatched area) protects rivers from stream capture, both by preventing backwards erosion of streams on the alluvial plain and by deflecting other offset streams. Once the ridge has been displaced sufficiently to expose the river the alluvial plain (t=1), either capture or autonomic adjustment can reset its offset.

Figure 9. Satellite imagery (©2011 Google; GeoEye; DigitalGlobe; Cnes/Spot Image) showing how the structure of KB 1 and KB 10 has affected stream courses and hence spacing. Dashed black lines show the location of the drainage divide and blue lines show river courses. (a) KB 1. Solid black lines represent topographic ridges formed by resistant beds. Rivers C and D have been forced to flow between these ridges, causing them to be more closely spaced than they otherwise would have been. (b) KB 10. Shaded areas represent blocks within the ridge that have deflected the main rivers, causing them to be abnormally widely spaced. (c) Three-dimensional view of the largest block in (b) showing its relative topographic height.

Figure 10. Schematic explanation of the relationship shown in Fig. 7b. Mean outlet spacing of main rivers is typically 3 times their mean offset, D. They can be captured by smaller rivers with spacing similar to D, which therefore control the maximum observed offset.

Walker and Allen, highlights:

Active right-lateral slip along the Kuh Banan Fault, Iran, offsets rivers by ≤3.5 km

River offset is less than total bedrock offset because of stream capture

Mean offset of the main rivers is one-third their mean drainage spacing

Offset rivers, drainage spacing and the record of strike-slip faulting:

the Kuh Banan Fault, Iran

Faye Walker*, Mark B. Allen

Department of Earth Sciences, University of Durham, Durham, DL1 3LE, UK

*Corresponding author.

e-mail: fayemousw@googlemail.com; m.b.allen@durham.ac.uk

ABSTRACT

This study concerns the ways in which rivers can record part, but not necessarily all, of strike-slip fault offset. The focus is the active right-lateral Kuh Banan Fault in eastern Iran, within the Arabia-Eurasia collision. Plate convergence has caused thrust and strike-slip faulting across SW Asia. The active slip rate of the Kuh Banan Fault is ~1-2mm/yr. Total displacement is ~5-7 km, as determined from offset geological markers and the length of a pull-apart basin. A component of thrusting has generated ~1 km of relief, which preserves the offset of rivers displaced laterally by the strike-slip motion. Ridge half-widths (W), and river outlet spacings along the fault (S) are related by the drainage spacing parameter R, where $R = W/S$. Published data for older, larger mountain ranges have extremely characteristic drainage spacing ($R = 2.1$). Drainage spacing along the Kuh Banan Fault has a mean value of 1.8 and is much more variable ($R = 1.1-3.1$), due to local structural complexities which have influenced river courses. Most river offsets along the Kuh Banan Fault are small (<100 m); the maximum observed offset (~3.5 km) is smaller than the total fault displacement of at least ~5 km. The most likely explanation for this discrepancy is stream capture, whereby reaches of rivers downstream of the fault are juxtaposed by fault slip against rivers upstream of the fault. In this way, offset of individual rivers is repeatedly reset to zero. Stream capture is influenced by outlet spacing such that the largest rivers can accumulate large offsets, while smaller, closely

spaced rivers are captured more often, inhibiting large offsets. The mean offset of the main rivers along the Kuh Banan Fault is one-third their mean drainage spacing, indicating that the spacing of smaller rivers controls the size of the maximum offset.

Keywords: strike-slip fault; river offset; Iran.

1. Introduction

Deformation within tectonically active regions has significant effects on river systems. Strike-slip faulting can result in the lateral offset of rivers, as well as other geological and geomorphic markers (Huang, 1993; Fu *et al.*, 2005; Fu & Awata, 2007; Cowgill; 2007; Cowgill *et al.,* 2009), while uplift causes incision and may result in the deflection of river channels, affecting drainage basin geometry. The pattern of stream offsets along a strike-slip fault can provide clues about its movement and the growth of fault-related topography and how this affects drainage development (Fu *et al.*, 2005; Jackson *et al.*, 1996). Offsets along strike-slip faults are known to increase with time due to repeated slip (Sylvester, 1988) so that the largest observed offset should equal the total fault displacement. This is generally thought to be the case for offsets of large rivers as well as more permanent geological markers (e.g. Westaway, 1994; Talebian & Jackson, 2002; Fu *et al.*, 2005; Fu and Awata, 2007). It is also possible to restore multiple smaller offsets (by matching channels on either side of the fault and finding the best-fitting configuration) to determine the total fault displacement, as has been shown for the Red River Fault in east Asia (~25 km offset; Replumaz *et al.*, 2001).

It has long been observed that there is a remarkable degree of regularity in the spacing of river outlets along mountain fronts, particularly in linear mountain ranges where the drainage runs transverse to the mountain front (Hovius, 1996; Talling *et al.*, 1997; Purdie & Brook, 2006). Hovius (1996) developed a quantitative method for documenting the regularity of drainage spacing in large-scale linear mountain belts (see section 3) using the half-width

2

of the range and the mean outlet spacing. He found that the ratio between these two values (drainage spacing ratio, *R*) was extremely consistent (between 1.91 and 2.23) for the 11 orogens studied, irrespective of age and climate. His method has since been applied to smaller, younger fault blocks (Talling *et al.*, 1997; Purdie & Brook, 2006), where outlet spacing was again found to be regular.

Drainage spacing has not previously been investigated at mountain range fronts affected by strike-slip faulting, where it may be affected by the fault movement and resultant complex topography. This study investigates the relationship between river systems, faulting and topography for the Kuh Banan Fault in eastern Iran (Fig. 1), which is an active strike-slip fault with relief across it, caused by a component of thrusting. Firstly, offsets at varying scales are documented, and possible controls affecting the size of offsets are considered. Secondly, drainage spacing on the Kuh Banan Fault is investigated, and properties influencing it are discussed.

2. Tectonic Setting

Active deformation in Iran is related to the Arabia-Eurasia collision, which causes ~25mm/yr of roughly north-south convergence at longitude ~56°E (Vernant *et al.*, 2004). The deformation occurs largely within a compact area delimited by the political borders of Iran (Walker *et al.* 2010), and is mostly accommodated in the compressional zones of the Zagros Mountains in the south, and the Alborz and Kopeh Dagh mountains in northern Iran (Fig. 1a). GPS studies suggest that ~10 mm/yr of convergence is taken up in the central Zagros (Tatar *et al.*, 2002).

The remaining shortening is accounted for by the northward movement of central Iran with respect to Afghanistan (Fig. 1a) at 16±2 mm/yr (Vernant *et al.*, 2004). This right-lateral shear is taken up on N-S to NW-SE strike-slip faults in eastern Iran (Meyer & Le Dortz, 2007) by both right-lateral slip and anticlockwise rotation (Walker & Jackson, 2004; Allen *et*

3

al., 2011), and on left-lateral faults north of 34°N trending between E-W and N70°E, which are thought to rotate in a clockwise direction (Jackson & McKenzie, 1984). The Arabia-Eurasia collision is thought to have undergone a significant reorganisation at 5±2 Ma (Allen *et al.*, 2004; Copley & Jackson, 2006), based on changes in deformation and sedimentation (e.g. Axen *et al.*, 2001; Westaway, 1994) and the time needed to extrapolate active slip rates to achieve the total fault slip (Allen *et al.*, 2004). Meyer & Le Dortz (2007) propose an earlier date of 8-22 Ma. These active faults in places postdate earlier patterns of deformation, some of which is related to the construction of the Turkish-Iranian plateau (Morley *et al.,* 2009; Mouthereau, 2011).

The Kuh Banan Fault is a ~180km long right-lateral strike-slip fault located east of the city of Zarand (Fig. 1b). It has a NNW-SSE trend, roughly parallel to other strike-slip faults in the region (Behabad, Jorjafk and Rafsanjan) (Allen *et al.*, 2011). Adjacent to the fault there is ~1 km of topography, which switches from the west to the east side of the fault trace towards its northern end, suggesting a reversal of fault plane dip. This topography indicates that there is a thrust component to the fault movement; however, the fault plane solution of the Bob Tangol earthquake in 1977 (Berberian *et al.*, 1979) indicates mainly strike-slip motion with only a small amount of thrusting. The Kuh Banan Fault therefore appears to have changed from being a thrust or oblique thrust fault to the dominantly strike-slip fault seen today (Walker *et al.*, 2010).

At its southern end, the Kuh Banan Fault is simple and linear, but to the north it becomes fragmented into several strands (Mahdavi, 1996). There are two possible pull-apart basins located at bends in the fault trace (Allen *et al.*, 2011) (Fig. 1b). Total fault offset is uncertain, although Berberian (2005) determined a minimum offset of 5 km based on the displacement of Cambrian and Jurassic strata. Since the length of a pull-apart basin may serve as a minimum estimate for total offset along a strike-slip fault (Mann *et al.* 1983), the length

of the southern pull-apart suggests that the minimum offset is ~7 km. The slip-rate of the Kuh Banan Fault is estimated at 1-2 mm/yr. This is based on stream offsets assumed to have formed since ~12±2 ka, when regional climate change resulted in widespread incision, and the fact that the fault does not perturb the regional GPS velocity field (Allen *et al*., 2011; Meyer & Le Dortz, 2007).

The Kuh Banan Fault is seismically active (Berberian *et al.*, 1979; Talebian *et al.*, 2006). Numerous earthquakes have been recorded (Fig. 1b), including the M_s 5.8 Bob-Tangol earthquake at 30.9ºN 56.6ºE on 19th December 1977 (Berberian *et al.*, 1979) and other large events in 1933 and 1978 on the northern section of the fault. Earthquakes have also occurred on nearby faults, including the Dahuiyeh thrust which ruptured in 2005 (Talebian *et al.*, 2006) and the Behabad fault (Ambraseys and Melville, 1982).

3. Methodology and data

High-resolution satellite imagery (acquired from Quickbird, SPOT and GeoEye-1 satellites and viewed in Google Earth) and Shuttle Radar Topography Mission (SRTM) digital topographic data were used in this study (Rodriguez *et al.*, 2005; Jarvis *et al.*, 2008). SRTM data have a specified vertical absolute accuracy of ≤16 m (Rodriguez *et al.* 2005). Gorokhovich and Voustianiouk (2006) found it ranged from 7.58±0.60 m to 4.07±0.47 m in two local case studies. Specific vertical relative accuracy is quoted as ≤10 m (Rodriguez *et al.* 2005).

Satellite images were used to measure the offset (parallel to the fault trace) and the drainage length (taken to be the distance from the point where the river crosses the fault trace to the source of the most distant tributary) of rivers along the Kuh Banan Fault. In order to accurately measure the offset, the upstream and downstream course of each river was projected onto the fault trace (Fu e*t al*., 2005) (Fig. 2a). Offsets in the opposite sense to fault movement can occur via stream capture (Fu *et al.*, 2005; Huang, 1993) (Fig. 2b), so to avoid

5

bias in the measurements apparent left-lateral offsets were also measured. Since the fault is right-lateral, however, these left-lateral offsets were not considered for the bulk of the study. The gradients of the largest rivers were measured from SRTM data in order to see how gradient varies across the fault.

The method devised by Hovius (1996) was then applied to rivers along the Kuh Banan Fault (Fig. 3). Due to the highly variable topography along the Kuh Banan Fault there is no simple, single main drainage divide, so the mountain range was divided into ten separate ridges (Fig. 1b) which formed local drainage divides. Each ridge was treated as a separate mountain range for the purpose of drainage spacing calculation. There are no wind or water gaps within these ridges. The outlet spacing (s) of adjacent catchments with trunk streams originating at the main drainage divide was measured, as was the ridge half-width (w), defined as the distance between the mountain front and the drainage divide (Fig. 4a). The means of these values were used to calculate the spacing ratio (R) for each ridge using the equation $R = W/S$, where W and S are the mean values of w and s. Spacing ratios for individual catchments were also determined and their mean (R') calculated for each ridge. Since R' is greatly affected by outliers and may not therefore be representative of the ridge as a whole, the value of R was used to characterise the drainage spacing of each ridge.

The ridges and folds used were often nonlinear, so the local half-widths (w_{local}) of individual catchments were averaged to get a more accurate measurement. Outlet spacing s was measured parallel to the mountain front and w was measured perpendicular to it (Fig. 4a). All rivers that originated within $0.1w_{local}$ of the main divide (henceforth referred to as "main rivers") were included, provided they did not merge with another main river further than $0.02w_{local}$ upstream of the mountain front, as specified by Hovius (1996). The standard deviations (σ_s and $\sigma_{r)}$ of S and R', respectively, were calculated. It was found that σ_s tends to

6

increase with the magnitude of S, so the ratio between S and σ_s ($\sigma\%$) was determined in order to better quantify the regularity of outlet spacing.

The sinuosity of each ridge and fold was calculated using the method devised by Keller & Pinter (1996) to see if there is a correlation between sinuosity and drainage parameters. Any such correlation would have to be accounted for in making further interpretations of the drainage data. First the total length of the mountain front between two points was measured and then this length was divided by the distance between those two points in a straight line. This process was then repeated for the ridge crest (Fig. 4b).

4. Results

4.1 River offsets

187 offset rivers were measured along the Kuh Banan Fault (see Appendix 1): 153 right-lateral (Figs. 5a-f) and 34 left-lateral (Figs. 5g & 6a). Right-lateral offsets range from 4 to 3478 m with a mean of 170 m. 104 of the rivers have offsets smaller than 100 m, and only 12 have offsets greater than 500 m. The largest (>1 km) offsets are typically located behind shutter ridges (i.e. ridges which have been displaced along the fault) (Fig. 5e). Left-lateral offsets are in general much smaller (Fig. 6a) ranging from 4 to 290 m, except for one extremely large offset of 2272 m (which appears to have been deflected by a shutter ridge). Several of the main rivers on ridges 1, 2, 3, 5 and 9 (see section 3; Fig. 3) have been offset (see appendix 2). The mean offset varies from 45m to 1097 m (Table 1). There is a positive correlation between offset (D) and drainage length (L). The line of best fit has an r^2 value of 0.79 and an equation of $L = 5.24D + 279$ (Fig. 6b). There are several clusters of offset length, at 0-50 m, 50-100 m, 100-200 m, 200-300 m, 350-500 m, and >500 m (Fig. 6c).

Fig. 6d shows that the gradient of rivers tends to decrease where the river is offset. This is due to the dominantly strike-slip movement of the fault. Each end of the offset is moved only laterally, not vertically, so that the elevations of the two points do not change

7

significantly with fault slip. Since the horizontal distance between them increases but the vertical distance remains the same, the gradient of the offset must decrease.

4.2 Drainage spacing

There is significant variability in half-width and spacing both between ridges and within each ridge (Table 1; Fig. 3; see appendix 2). W varies between 364 m and 6122 m; within a single ridge w can vary by up to 4 km. S ranges from 173 m to 5652 m. Spacing is highly irregular in six of the ridges ($\sigma\%$ is between 0.59 and 0.9).

Variation in spacing ratio R is also large, varying between 1.1 and 3.1. The mean ratio is 1.8, smaller than the value of 2.1 determined by Hovius (1996) but within his range of values. Spacing ratio also varies significantly within ridges 3, 4, 5 and 7 (σ_r is between 1.45 and 5.73), but is more consistent within the others (Table 1). There is a clear correlation between the half-width of the ridge and the outlet spacing (Fig. 7a; see section 4.2). A relationship also exists between the spacing of the main rivers on several ridges and their mean offset (Fig. 7b). The equation of the regression line is $S = 3.17D + 193$, and the r^2 value is 0.91, showing that the mean offset is ~3 times smaller than the mean spacing. KB 1 was not included in Fig. 7b because it has only one offset.

4.3 Sinuosity

Sinuosity is variable along the Kuh Banan Fault. Mountain fronts are typically less sinuous than crests. No correlation exists between sinuosity (of either mountain fronts or crests) and either outlet spacing regularity ($\sigma\%$) or spacing ratio R (Figs. 7d-e).

4.4 Uncertainty

Given that the tools and imagery used for the measurements outlined in section 3 are accurate to within 0.5%, uncertainty in these results arises almost exclusively from human inaccuracy and is therefore extremely difficult to quantify. The most inaccurate measurements

8

are the ridge half-widths, since the precise location of the crest and mountain front is often unclear, and the drainage lengths, because it can be difficult to determine the location of the source of a river (especially for larger catchments). Offset and outlet spacing measurements are also subject to error, but repeated measurements show that this error is likely to be less than ~5%. This could be reduced by measuring each offset and outlet spacing three or more times, but limited time made this approach unfeasible.

Another potential source of error is the fact that *w* was measured horizontally across each ridge in this study, whereas Hovius (1996) measured the diagonal widths of his mountain ranges. However, the difference between horizontal and diagonal widths in this area is small (<5%) and hence the results of the two studies can still be directly compared. In summary, uncertainty is not formally quantified in this study. It is expected that total error will be on the order of a few percent and therefore is not significant.

5. Discussion

5.1 River offsets

The most striking aspect of the Kuh Banan Fault is the number of river offsets that are present along its length (see Appendix 1), as previously reported by Berberian *et al.,* (1979). A brief examination shows that other strike-slip faults in the region do not preserve nearly as many, despite having similar number of drainages. The reason for this is not known for certain, but may be related to the rates of uplift and lateral movement on the Kuh Banan Fault. Both of these are required in order to create and preserve offsets, since a fault with only vertical movement would create topography but no offsets; whereas a purely strike-slip fault creates no topography, allowing rivers to meander freely across the fault trace and thus preserving no offsets. The Kuh Banan Fault is thought to have a greater slip rate than the similarly-uplifted Jorjafk fault (estimated slip rate <1 mm/yr); it also has higher topography (suggesting a greater rate of uplift) than the nearby Behabad fault, which slips at a similar rate

9

(Fig. 1b) (Allen *et al.*, 2011). It is therefore probable that the movement of the Kuh Banan Fault is simply better suited to preserving river offsets than that of nearby faults, by virtue of its component of dip slip motion. It is possible that thrust motion and surface uplift in the region slightly preceded strike-slip deformation (Walker *et al.*, 2010), implying that at least the larger scale drainage patterns also pre-date the strike-slip.

The observation that uplift is required for offset preservation explains the distribution of offsets seen along the Kuh Banan Fault. Most offsets are found on the uplifted southern section of the fault, with very few being observed towards the northern end which is located within an alluvial plain (Fig. 1b).

The key observation highlighted by Fig. 6b is a lack of river offsets along the Kuh Banan Fault comparable to the bedrock offset. The presumed age of the fault (~5 Ma; Allen *et al.*, 2004) combined with the estimated slip rate of 1-2 mm/yr (Allen *et al.*, 2011) suggests that there should be offset on the order of 5-10 km. Even if slip rate was lower in the past, or the fault is younger than 5 Myr, the minimum total displacement of ~5-7 km determined by Berberian (2005) and this study (see section 2) is greater than the maximum river offset of ~3.5 km.

One possible explanation for this discrepancy is climate change, resulting in changes in base-level. If base-level rose sufficiently to encroach on the margin of the topography adjacent to the Kuh Banan Fault, the rivers would no longer flow along the fault but straight into the newly-formed lake. This would obliterate all offset channels so that when base level fell and the lake drained away the rivers would flow straight across the fault trace (Fig. 8a). Present-day base level is in the region of Zarand (Fig. 1b), at an elevation of ~1650 m. By contrast the elevation of the mountain front is ~2000 m, meaning that a base-level rise of ~350 m would be required. This is unfeasible, as there are numerous lower-elevation spill-

10

points around the edges of the regional drainage basin which would prevent the rising water reaching the Kuh Banan mountain front.

A widespread fall in base-level, on the other hand, would result in increased river incision, which acts to straighten stream courses (Huang, 1993). However, this would not significantly decrease offsets, especially for larger rivers and displacements, and cannot therefore account for the difference between the 5-7 km geological offset and the 3.5 km river offset.

An extremely arid climate would cause the rivers to completely dry up. If they were dry for long enough continued fault movement would further offset the valleys on either side of the fault. Without river flow and incision the near-zero gradient (Fig. 6d) along the fault could conceivably break the connection between the valleys. When the rivers resumed flow they would have to find a new downstream course, invariably resulting in a smaller apparent offset than had previously existed (Fig. 8b). The valleys would need to be separated by several hundred metres to break the connection, however, and with a slip rate of 2 mm/yr the rivers would have to be dry for >100 ka. It is highly unlikely that the climate of eastern Iran was sufficiently arid for such a long period of time: Walker and Fattahi (2011) demonstrated the late Pleistocene/Holocene variability of east Iranian climate, on timescales far shorter than 100 ka.

A more likely explanation is stream capture (Fig. 2b; see section 3). This is a common process on the Kuh Banan Fault as shown by the occurrence of left-lateral offsets (Fig. 5g). In some cases it is possible to identify the old (right-lateral) course of a river that has recently been captured (Fig. 5g), showing that this is a viable mechanism for resetting the apparent offset of a stream (as suggested by Replumaz *et al.*, 2001). While these instances are rare and mostly confined to smaller streams, the same process will also occur with larger rivers. Once the river was captured and the offset reset, further fault slip would result in a new, smaller

11

right-lateral offset (Fig. 2b). Streams on the alluvial plain may also be capable of capture through backwards erosion of their headwaters. Stream capture is likely to be promoted by the shallow river gradient along the fault trace, as this makes the original course more difficult to maintain. This process could account for the gap between the largest (~3.5 km) offset and the next largest (~1.6 km): the larger occurs on an unusual section of the fault, where there are no rivers nearby that could capture it (Fig. 5b), while the other rivers are surrounded by streams.

Finally, a river may alter its own course in order to take advantage of an easier pathway, thereby reducing its apparent offset. This is possible if the gradient along the fault becomes low enough to cause spontaneous rerouting of the river, but may not occur under normal conditions since incision and the thrust component to the fault's movement help maintain an above-zero gradient. If, however, the region experienced exceptional levels of rainfall which caused flooding, a river may burst its banks in a manner analogous to levee breach, and erode a new pathway onto the alluvial plain (Fig. 8c). This new route would have a steeper gradient than the offset section of the river, so that when water levels fell the stream would make use of the new channel and abandon the old one. This process is instantaneous in geological terms, and hence is difficult to identify unless it is being observed at the time of breach. It is not possible therefore to determine whether this has occurred on the Kuh Banan Fault. The shallow gradient along the fault trace may also make it more likely for a river to significantly alter its course in response to a blockage, such as a landslide.

The common coexistence of shutter ridges and large (>1 km) displacements (see section 4), suggests that the ridges aid the formation of large offsets, by protecting against stream capture. It is unlikely that these ridges have artificially enlarged the offset as rivers are clearly displaced by the fault before encountering the ridge (Fig. 5e). This protection is twofold: firstly, streams on the alluvial plain would have to erode through the ridge; secondly, the topography would deflect the course of any other offset streams that might be capable of

12

capture (Fig. 8d). The few large offsets not protected by a shutter ridge are invariably deeply incised into the bedrock, which provides similar (and longer-lasting) protection from stream capture.

These effects would persist only for as long as the shutter ridge was located opposite the river. As soon as it is displaced enough to leave part of the river open to the alluvial plain, the river is again vulnerable to capture, which is why offsets larger than a few kilometres are not produced by shutter ridges. This may explain the gap between the two largest offsets, because the ~3.5 km offset is protected by a ridge much longer than any others on the Kuh Banan Fault (Fig. 5a).

Shutter ridges may also facilitate course adjustments of rivers in response to the shallow gradient along the fault. Once the shutter ridge is displaced enough to leave the upstream section of the river open to the alluvial plain, a much easier pathway for the river would exist by flowing past the end of the shutter ridge rather than all the way around it (Fig. 8d).

The relationship observed in Fig. 6b, where drainage length has a positive correlation with offset, would be expected even if stream capture or other rerouting processes did not operate, because drainage length and offset both increase with the age of a river. Many of the offsets are likely to have been modified, however, so it interesting that the correlation between drainage length and offset exists. This indicates that there is a relationship between the size of a river and how often it is captured, assuming stream capture is the dominant process limiting offset size. Smaller rivers are never offset by large amounts (and are presumably captured before large offsets can form) while the larger rivers can accumulate a larger offset before they are captured. This could be because drainage spacing controls river capture (as postulated by Huang, 1993) and, ultimately, offset. A river can never be offset by a greater amount than the distance to the next stream capable of capture, since capture will

13

occur and the offset will be reset as soon as the two rivers are close enough (Fig. 2b). Smaller

rivers occur close together, and therefore capture occurs before the offset can reach more than

a few tens or hundreds of metres; whereas the larger rivers are much more widely spaced (and

presumably can only be captured by rivers of a comparable size) allowing the offsets to grow.

Capture occurring at different scales may account for the clustering seen in Fig. 6c.

It is interesting that it does not seem to matter whether the rivers are perennial or not;

there is no clear jump in the ratio data which might correspond to a switch from ephemeral or

intermittent to perennial drainage (Fig. 6).

5.2 Drainage spacing and sinuosity

The high values of σ_r (Table 1) show that the spacing ratio of individual drainage

basins is highly variable. Generally, however, there is a predominance of values of around 2 −

high σ_r values tend to be due to a small number of basins with anomalously high or low ratios.

This suggests that the relationship between W and S applies to individual drainage basins as

well as entire drainage networks.

There is no clear systematic variation in R with location on the Kuh Banan Fault,

although both the highest and lowest values are found at the ends of the fault trace. In general

lower R-values are found on the northern half of the fault (Fig. 1b; Table 1). The highest value

of R (3.2) is found on ridge KB 1 at the southern end of the fault, where the topography is

dominated by a pair of steeply-plunging folds (Fig. 9a). Several stratigraphic units within

these folds are resistant to erosion and form distinct topographic ridges. These have

influenced the courses of the main rivers resulting in long and narrow drainage basins. The

structure of the mountain range in this location has therefore produced a closer spacing than

would have existed otherwise.

14

Topography seems to have exerted a similar control on ridge KB 10 with the lowest *R*-value of 1.1. In this case however there are several topographically high blocks that have clearly deflected the main rivers (Figs. 9b-c). These blocks are deeply incised by smaller streams and are therefore unlikely to be caused by a resistant lithology, but may be a result of differential uplift within the ridge. The deflection results in very broad drainage basins, and hence a wider-than-typical outlet spacing. A similar process appears to have occurred on other ridges with anomalously low (<1.5) spacing ratios.

Talling *et al.* (1997) determined that *S* was irregular for fault blocks with sinuous mountain fronts. The results of this study however suggest that this is not the case (Figs. 7d-e), and that sinuosity of either mountain fronts or ridge crests has no effect on drainage spacing.

Hovius (1996) found a mean spacing ratio of 2.1, larger than that determined for the Kuh Banan ridges in this study (1.8). This suggests that drainages along the Kuh Banan Fault tend to be more widely spaced than those in the larger mountain belts studied by Hovius (1996). The difference between the mean *R* value for the Kuh Banan Fault and the larger mountain belts is intriguing, especially given the general consistency within Hovius's (1996) results. This is unlikely to be due to differences in ridge half-width, even though the mountain belts are $1 - 2$ orders of magnitude larger than the Kuh Banan ridges (Fig. 7c), as the smallest ridge measured for Kuh Banan (*W* = 364 m) has a ratio of 2.1. A more likely possibility is that variable topography (Fig. 9) has resulted in a lower spacing ratio. There is no evidence to suggest that the strike-slip movement of the Kuh Banan Fault has had any effect on the spacing ratio.

Talling *et al.* (1997) investigated drainage spacing for fault blocks in the United States and determined an average ratio of 2.5, with individual blocks varying between 1.4 and 4.1, a far greater range than that of Hovius (1996). They concluded that this was due to local factors

such as uplift rate, precipitation and lithology, and noted that it is enigmatic why such factors do not carry through to the larger mountain ranges studied by Hovius (1996), or even the Kuh Banan Fault described in this study. The overall aridity of eastern Iran means that variation in precipitation patterns cannot be an important control and it has already been determined that lithology has no effect on spacing ratio, but variable uplift may have caused the structural complexity resulting in low spacing ratios on the Kuh Banan Fault.

Purdie and Brook (2006) looked at drainage spacing on the Ruahine Range in New Zealand. They found an extremely low R value of 1.31, and interpreted this as being due to fault splays which resulted in widening of drainage basins. This is not the case for the Kuh Banan Fault, but also suggests that structural complexity can have a major effect on drainage spacing on small scales.

5.3 Relationship between drainage spacing and offset

Given the hypothesis that drainage spacing controls how often stream capture occurs (see section 5.1), there should be a relationship between the mean observed offset of main rivers on the Kuh Banan Fault and the outlet spacing of those rivers (assuming that only streams of similar or larger size are capable of capturing each other). We would expect the mean offset to be close to, but never more than, the mean outlet spacing. Table 1 clearly shows that not only is the mean offset consistently much smaller than the mean outlet spacing, but that the maximum offset is also much smaller. The offset on ridge 7 is much more comparable to the mean spacing than for other ridges. It is, however, based on restoration of a beheaded alluvial fan (Fig. 5f) and hence is not affected by stream capture. At first sight, this suggests that outlet spacing cannot control the maximum offset observed on the fault. However, the consistent relationship shown in Fig. 7b, where the mean spacing is ~3 times larger than the mean offset for all ridges, strongly indicates that offset size is related to drainage spacing by this scale-independent ratio, as shown schematically in Fig. 10.

16

6. Conclusions

Right-lateral movement of the Kuh Banan Fault has resulted in the formation of numerous river offsets (Fig. 6). The slip rate and uplift of the Kuh Banan Fault allow good preservation of offsets along much of the fault trace (Fig. 5). Abandoned channels downstream of the fault trace are, however, easily eradicated through alluvial fan deposition, making it impossible to perform offset reconstructions to determine the fault's total displacement.

Although the total displacement of the fault is uncertain, minimum values of 5-7 km have been determined from geological offsets (Berberian, 2005) and the length of pull-apart basins (this study). The maximum observed river offset of ~3.5 km is therefore lower than the total offset. Several hypotheses have been proposed to explain this relationship, including climate change (resulting in base level rise, river incision or complete aridification of the region, depending on the climatic shift), stream capture, and gradient-related adjustments of stream profile (Fig. 8). The various climate-change hypotheses are rejected on the basis of observational and theoretical evidence: spill points at the edges of the regional drainage basin would prevent base level from reaching the Kuh Banan Fault; river incision would not substantially reduce large offsets; and the region would have to be completely dry for an unfeasibly long period of time in order to separate the upstream and downstream channels and cause changes in stream course. Adjustments of streams related to the shallow gradient of the fault may be effective under special circumstances but are unlikely to occur normally. Stream capture is therefore the favoured mechanism for reducing the size of apparent offsets. Stream capture appears to be controlled by drainage spacing such that smaller, closely-spaced rivers are only offset by <100 m before being captured, while larger, more widely-spaced rivers can accumulate much larger offsets. Shutter ridges encourage formation of large offsets through protection from stream capture and prevention of autonomic river adjustments.

17

Drainage spacing ratios of the Kuh Banan Fault are highly variable (Fig. 7) with a mean (1.8) significantly smaller than that determined by Hovius (1996) for larger ranges (2.1). This is attributed to structural complexity and resultant topographic variation deflecting rivers and affecting drainage basin shapes on smaller scales. The lateral movement of the Kuh Banan Fault does not appear to significantly affect the spacing or geometry of drainage basins.

While drainage spacing seems to control the mean offset of rivers along the Kuh Banan Fault the relationship is not simple. Main rivers can be captured by smaller streams (not originating at the main drainage divide) such that the size of their offset never approaches their spacing (mean spacing is typically 3 times larger than the mean offset; Fig. 10).

Although both river offsets and drainage spacing have been investigated previously, this study is the first to have combined the two to determine the effect that spacing has on offset. Further investigation utilising knowledge of river dynamics is needed to establish the exact relationship.

Acknowledgements

References

Allen, M. B., Kheirkhah, M., Emami, M. H., Jones, S. J., 2011. Right-lateral shear across Iran and kinematic change in the Arabia-Eurasia collision zone. Geophys. J. Int., 184, 555-574.

Allen, M., Jackson, J., Walker, R., 2004. Late Cenozoic reorganization of the Arabia-Eurasia collision and the comparison of short-term and long-term deformation rates. Tectonics, 23, TC2008, doi: 10.1029/2003TC001530.

Ambraseys, N. N., Melville, C. P., 1982. A history of Persian earthquakes. Cambridge University Press, New York, pp. 164-166.

Axen, G. J., Lam, P. S., Grove, M., Stockli, D. F., Hassanzadeh, J., 2001. Exhumation of the west-central Alborz Mountains, Iran, Caspian subsidence, and collision-related tectonics. Geology, 29, 559-562.

Berberian, M., Asudeh, I., Arshadi, S., 1979. Surface rupture and mechanism of the Bob-Tangol (Southeastern Iran) earthquake of 19 December 1977. Earth Planet. Sci. Lett., 42, 456-462.

Berberian, M., 2005. The 2003 Bam Urban Earthquake: A Predictable Seismotectonic Pattern Along the Western Margin on the Rigid Lut Block, Southeast Iran. Earthq. Spectra, 21 (S1), S35-S99.

Copley, A., Jackson, J., 2006. Active tectonics of the Turkish-Iranian Plateau. Tectonics, 25, TC6006, doi: 10.1029/2005TC001906.

Cowgill, E., 2007. Impact of riser reconstructions on estimation of secular variation in rates of strike-slip faulting: Revisiting the Cherchen River site along the Altyn Tagh Fault, NW China. Earth Planet. Sci. Lett., 254, 239-255.

19

Cowgill, E., Gold, R.D., Chen, X.H., Wang, X.F., Arrowsmith, J.R., Southon, J., 2009. Low Quaternary slip rate reconciles geodetic and geologic rates along the Altyn Tagh fault, northwestern Tibet. Geology, 37, 647-650.

Fu, B., Awata, Y., 2007. Displacement and timing of left-lateral faulting in the Kunlun Fault Zone, northern Tibet, inferred from geologic and geomorphic features. J. Asian Earth Sci., 29, 253-265.

Fu. B., Awata, Y., Du, J., He, W., 2005. Late Quaternary systematic stream offsets caused by repeated large seismic events along the Kunlun fault, northern Tibet. Geomorphology, 71, 278-292.

Gorokhovich, Y., Voustianiouk, A., 2006. Accuracy assessment of the processed SRTM-based elevation data by CGIAR using field data from USA and Thailand and its relation to the terrain characteristics, Remote Sens. Environ., 104, 409-415.

Hovius, N., 1996. Regular spacing of drainage outlets from linear mountain belts. Basin Res., 8, 29-44.

Huang, W., 1993. Morphologic patterns of stream channels on the active Yishi Fault, southern Shandong Province, Eastern China: implications for repeated great earthquakes in the Holocene. Tectonophysics, 219, 283-304.

Jackson, J., Norris, R., Youngson, J., 1996. The structural evolution of active fault and fold systems in central Otago, New Zealand: evidence revealed by drainage patterns. J. Struct. Geol., 18, 217-234.

Jackson, J., McKenzie, D., 1984. Active tectonics of the Alpine-Himalayan belt between Turkey and Pakistan. Geophys. J. Roy. Astr. Soc., 77, 185-264.

20

Jarvis, A., Reuter, H.I., Nelson, A., Guevara, E., 2008. Hole-filled SRTM for the globe Version 4, available from the CGIAR-CSI SRTM 90m Database (http://srtm.csi.cgiar.org).

Keller, E. A., Pinter, N., 1996. Active Tectonics: Earthquakes, Uplift, and Landscape. Prentice Hall, New York, pp. 138.

Mahdavi, M. A., 1996. Geological Quadrangle map of Iran, 1:250,000 scale, sheet NH 40.2 (Ravar), Geological Survey of Iran.

Mann, P., Hempton, M. R., Bradley, D. C., Burke, K., 1983. Development of pull-apart basins. J. Geol., 91, 529-554.

Meyer, B., Le Dortz, K., 2007. Strike-slip kinematics in Central and Eastern Iran: Estimating fault slip-rates averaged over the Holocene. Tectonics, 26, TC5009, doi: 10.1029/2006TC002073.

Morley, C.K., Kongwung, B., Julapour, A.A., Abdolghafourian, M., Hajian, M., Waples, D., Warren, J., Otterdoom, H., Srisuriyon, K., Kazemi, H., 2009. Structural development of a major late Cenozoic basin and transpressional belt in central Iran: The Central Basin in the Qom-Saveh area. Geosphere, 5, 325-362.

Mouthereau, F., 2011. Timing of uplift in the Zagros belt/Iranian plateau and accommodation of late Cenozoic Arabia–Eurasia convergence. Geol. Mag., 148, 726-738.

Purdie, H., Brook, M., 2006. Drainage spacing regularity on a fault-block: A case study from the eastern Ruahine Range. New Zeal. Geogr., 62, 97-104.

Replumaz, A., Lacassin, R., Tapponnier, P., Leloup, P. H., 2001. Large river offsets and Plio-Quaternary dextral slip rate on the Red River fault (Yunnan, China). J. Geophys. Res., 106 (B10), 819-836.

Rodriguez, E., Morris, C.S., Belz, J.E., Chapin, E.C., Martin, J.M., Daffer, W., Hensley, S., 2005. An assessment of the SRTM topographic products, Jet Propulsion Laboratory, Pasadena, California, Technical Report D-31639, 1-143.

Sylvester, A. G., 1988. Strike-slip faults. Geol. Soc. Am. Bull., 100, 1666-1703.

Talebian, M., Biggs, J., Bolourchi, M., Copley, A., Ghassemi, A., Ghorashi, M., Hollingsworth, J., Jackson, J., Nissen, E., Oveisi, B., Parsons, B., Priestley, K., Saiidi, A., 2006. The Dahuiyeh (Zarand) earthquake of 2005 February 22 in central Iran: reactivation of an intramountain reverse fault. Geophys. J. Int., 164, 137-148.

Talebian, M., Jackson, J., 2002. Offset of the Main Recent Fault of NW Iran and implications for the late Cenozoic tectonics of the Arabia-Eurasia collision zone. Geophys. J. Int., 150, 422-439.

Talling, P. J., Stewart, M. D., Stark, C. P., Gupta, S., Vincent, S. J., 1997. Regular spacing of drainage outlets from linear fault blocks. Basin Res., 9, 275-302.

Tatar, M., Hatzfeld, D., Martinod, J., Walpersdorf, A., Ghafori-Ashtiany, M., Chéry, J., 2002. The present-day deformation of the central Zagros from GPS measurements. Geophys. Res. Lett., 29 (19), 1927, doi: 10.1029/2002GL015427.

Vernant, P., Nilforoushan, F., Hatzfeld, D., Abbassi, M. R., Vigny, C., Masson, F., Nankali, H., Martinod, J., Ashtiani, A., Bayer, R., Tavakoli, F., Chéry, J., 2004. Present-day crustal deformation and plate kinematics in the Middle East constrained by GPS measurements in Iran and northern Oman. Geophys. J. Int., 157, 381-398.

Walker, R., Jackson, J., 2004. Active tectonics and late Cenozoic strain distribution in central and eastern Iran. Tectonics, 23, TC5010, doi: 10.1029/2003TC001529.

Walker, R. T., Talebian, M., Saiffori, S., Sloan, R. A., Rasheedi, A., MacBean, N., Ghassemi, A., 2010. Active faulting, earthquakes and restraining bend development near Kerman city in southeastern Iran. J. Struct. Geol., 32, 1046-1060.

Walker, R.T., Fattahi, M., 2011. A framework of Holocene and Late Pleistocene environmental change in eastern Iran inferred from the dating of periods of alluvial fan abandonment, river terracing, and lake deposition, Quat. Sci. Rev., 30, 1256-1271.

Westaway, R., 1994. Present-day kinematics of the Middle East and eastern Mediterranean. J. Geophys. Res., 99 (B6), 12071-12090.

Figure Captions

Figure 1. Location maps. (a) Location of the study area (satellite image ©2011 Google; LeadDog Consulting; Europa Technologies). Black lines are the national borders of Iran. Arrow shows the movement of Iran relative to Afghanistan. (b) Map showing major faults of the Kuh Banan region overlain on an SRTM image (Allen *et al.*, 2011). Numbers refer to the locations of ridges used for drainage spacing (Fig. 3 & Table 1). Sub-parallel right-lateral strike-slip faults are dominant and associated with significant topography due to a component of thrusting. Two pull-apart basins are located at bends in the Kuh Banan Fault, located between ridges KB5 and KB6 and KB9 and KB10. Earthquake focal mechanisms from Talebian *et al.* (2006) for the 1977 and 2005 events, and the Harvard catalogue (http://www.globalcmt.org; records filtered for >70% double-couple solutions) for the 2007 event. Other epicentres (M_w>4.5), given by white circles, are from the National Earthquake Information Center (NEIC) catalogue (http://earthquake.usgs.gov/earthquakes/) and Ambraseys and Melville (1982).

Figure 2. Form of river channels across a right-lateral strike-slip fault. (a) Measurement of stream offset across the fault trace. (b) Schematic diagram showing stream capture and the resulting left-lateral (opposite sense to the fault movement) offset (t=1). Further fault movement causes evolution of the left-lateral offset back into a smaller right-lateral offset (t=3).

Figure 3. Drainage basins along ridges used in drainage spacing calculations. "KB #" refers to ridges on the Kuh Banan Fault. Redrawn from satellite imagery. Scale bars represent a horizontal distance of 1 km and arrows indicate northward direction. Location numbers refer to those given in Table 1 and Figs. 1b-c.

Figure 4. Drainage spacing and sinuosity methodologies. (a) Schematic view of drainage basins on a ridge, showing the parameters used to calculate drainage spacing (after Hovius,

24

1996). Local half-width (w_1 and w_2) of each adjacent river was measured from the mountain front to the ridge crest, perpendicular to the mountain front, and averaged to give the ridge half-width (*w*). Outlet spacing (*s*) between adjacent drainage outlets was measured in a straight line parallel to the mountain front. (b) Schematic of a mountain front, showing the parameters used to calculate sinuosity. The total length of the mountain front, shown in bold, is divided by the length in a straight line to give the sinuosity.

Figure 5. SRTM and satellite images (©2011 Google; GeoEye; DigitalGlobe; Cnes/Spot Image) of river offsets along the Kuh Banan Fault. White arrows highlight the fault trace. (a) The largest offset is ~3.5 km long. (b) Smaller offset clearly showing the position of the Kuh Banan Fault. (c) The smallest offsets are just a few metres. These streams are offset by 14 m and 7 m. (d) Four streams with ~70m offset. Offset reconstruction matches the channels A, B, C and D with the valleys A', B', C' and D'. (e) 3D view of an offset behind a shutter ridge. (f) Beheaded alluvial fan (hatched area). The dotted line shows the river likely to have formed the fan.   (g) Left-laterally offset stream. Stream *A* has recently been captured and now flows into stream *B*, leaving a dry gulley, *C* (dashed white line), where the original stream course lay.

Figure 6. Graphical representation of offsets on the Kuh Banan Fault. (a) Plot comparing the number and sizes of right lateral vs. left lateral offsets. Right-lateral offsets dominate. (b) Plot showing the correlation between drainage length and offset for right-lateral offsets.
(c) Enlarged section of (b), showing detail of offsets smaller than 500m. Clusters occur at 0-50 m, 50-100 m, 100-200 m, 200-300 m and 350-500 m. (d) Gradients of large rivers along the Kuh Banan Fault, derived from SRTM data. The gradient decreases as the rivers cross the fault trace.

Figure 7. Graphs of drainage spacing and sinuosity. (a) Plot of ridge half-width (*W*) against outlet spacing (*S*). (b) Plot of the mean spacing of main rivers against their mean offset. (c)

25

Points in (a) superimposed on the plot from Hovius (1996). Regression line and red points are from Hovius (1996). (d) Sinuosity of ridges compared to outlet spacing regularity. (e) Sinuosity of ridges compared to spacing ratio.

Figure 8. Diagrams illustrating possible mechanisms for reducing the apparent stream offset. Dashed lines show abandoned valleys. See text for details. (a) Rising base level creates a lake with its margin along the Kuh Banan Fault (t=1), eradicating offsets (t=2). (b) Aridification of the region causes the stream to dry up (t=1). Continued fault movement breaks the connection between the dry valleys on either side of the fault (t=2), so that when the stream resumes flow it must find a new route across the fault (t=3). (c) Flooding of a river results in erosion of a new channel (t=1). When river levels fall back to normal this pathway is utilized because it has a steeper gradient than the offset (t=2). (d) Shutter ridge (hatched area) protects rivers from stream capture, both by preventing backwards erosion of streams on the alluvial plain and by deflecting other offset streams. Once the ridge has been displaced sufficiently to expose the river the alluvial plain (t=1), either capture or autonomic adjustment can reset its offset.

Figure 9. Satellite imagery (©2011 Google; GeoEye; DigitalGlobe; Cnes/Spot Image) showing how the structure of KB 1 and KB 10 has affected stream courses and hence spacing. Dashed black lines show the location of the drainage divide and blue lines show river courses. (a) KB 1. Solid black lines represent topographic ridges formed by resistant beds. Rivers C and D have been forced to flow between these ridges, causing them to be more closely spaced than they otherwise would have been. (b) KB 10. Shaded areas represent blocks within the ridge that have deflected the main rivers, causing them to be abnormally widely spaced. (c) Three-dimensional view of the largest block in (b) showing its relative topographic height.

Figure 10. Schematic explanation of the relationship shown in Fig. 7b. Mean outlet spacing of main rivers is typically 3 times their mean offset, D. They can be captured by smaller rivers with spacing similar to D, which therefore control the maximum observed offset.

Table 1. Morphological data for ridges along the Kuh Banan Fault. KB = Kuh Banan. Numbers correspond to those in Figs. 1b and 1c. See Fig. 3 for sketches. S = mean outlet spacing. W = ridge/fold half-width. R' = mean spacing ratio of individual basins. $R = W/S$. σ_s and σ_r = standard deviations of S and R, respectively.

Ridge /Fold	Mean offset (m)	Maximum offset (m)	S (m)	σ_s (m)	$\sigma\%$	W (m)	R'	σ_r	Number of rivers	R	Crest Sinuosity	Front Sinuosity
KB 1	1015	1015	1683	212	0.13	5230	3.13	0.23	4	3.11	1.368	1.192
KB 2	540	1526	1318	384	0.29	2722	2.22	0.80	6	2.07	1.081	1.004
KB 3	1097	1541	3805	3429	0.90	5448	2.33	2.00	3	1.43	1.257	1.038
KB 4	N/A	N/A	173	88	0.51	364	2.81	1.72	22	2.10	1.033	1.093
KB 5	259[1]	358	1788	1153	0.64	3565	4.49	5.73	6	1.99	1.303	1.158
KB 6	N/A	N/A	1779	1277	0.72	2399	1.76	0.77	7	1.35	1.179	1.168
KB 7	N/A	N/A	349	291	0.83	472	2.21	1.45	9	1.35	1.078	1.096
KB 8	N/A	N/A	704	207	0.29	848	1.29	0.40	5	1.20	1.117	1.039
KB 9	45	64	232	136	0.59	598	3.08	1.45	19	2.58	1.090	1.032
KB 10	N/A	N/A	5652	4199	0.74	6122	1.41	0.67	4	1.08	1.234	1.174
Kuh Banan Fault Mean			**1748**	1138	0.56	**2777**	2.47	1.52		**1.83**	1.174	1.099

1. This offset value differs to that plotted in Fig. 7b (which is 356 m) because two of the offset rivers occupied a highly anomalous part of the ridge. It was decided not to include them in Fig. 7b for simplicity of interpretation.

Figure
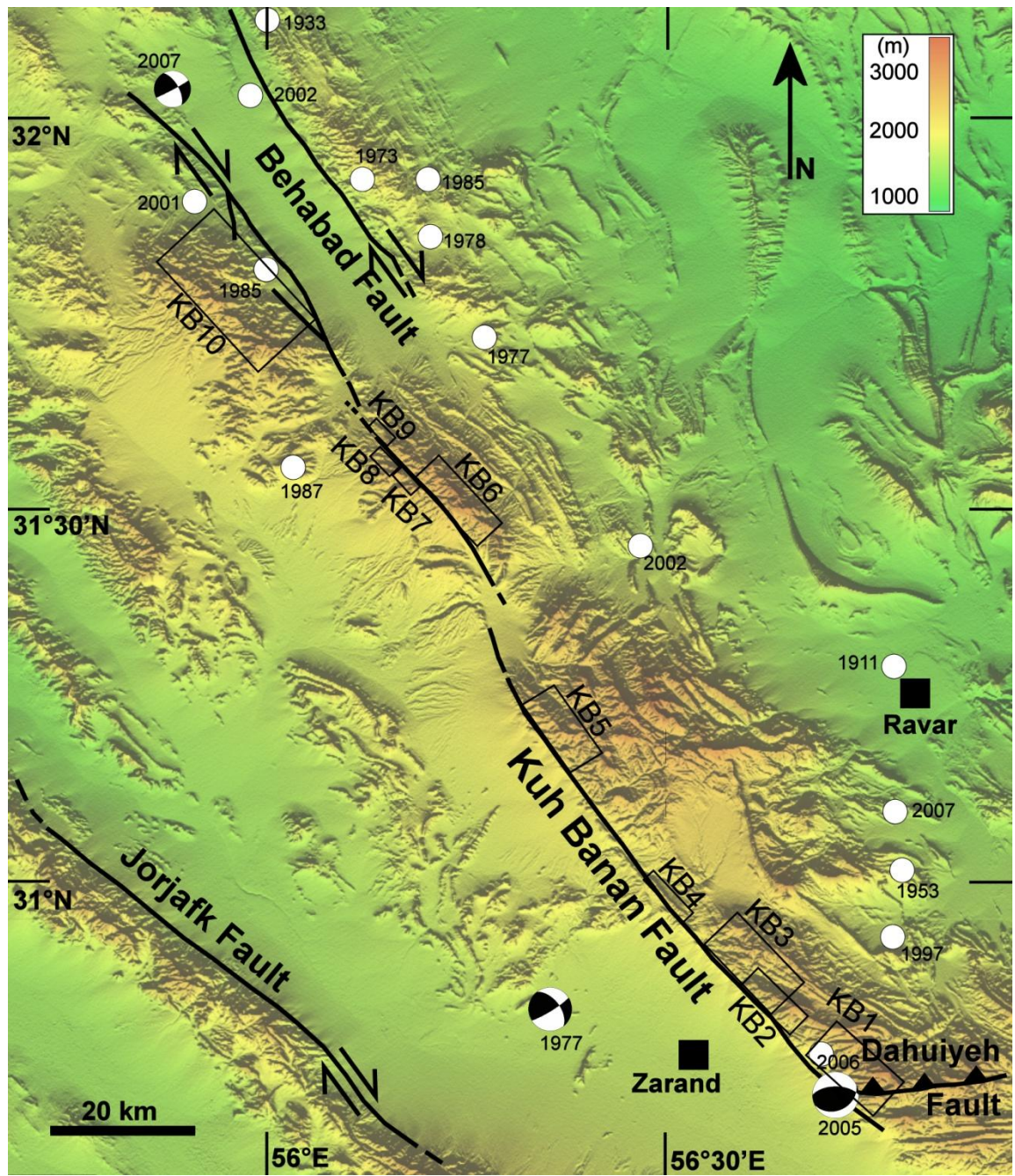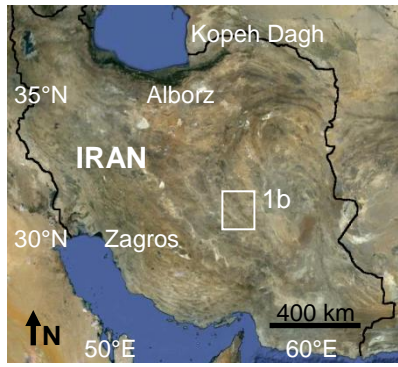
Figure 1

Figure 2

a

b

Figure

Figure 3

Key

Ridge crest
Mountain front
River used in study
Alluvial plain/fans
Source of main river

Figure 3 cont.

Figure

Figure 4

a

b

Figure 5

a — 3.5 km — 31°04' N 56°27; E

b — 250 m — 30°52'55" N 56°37'30" E

c — 30°56'16" N 56°34'07" E — 10 m

d — 31°00'34" N 56°30'12" E — C, D, B, A, D', C', B', A' — 50 m

e — 100 m — 30°58'14" N 56°32'14" E

f — 300 m — 30°47' N 56°42' E

g — 30°56'09" N 56°34'14" E — A, B, C — 10 m

Key

Channel downstream of fault.

Channel upstream of fault

Figure 6

Figure 7

Figure

Figure 8

Figure 9

a

30°48' N
56°42' E

D

C

A   B

N   1 km

b

31°47' N
55°58' E

Ashterk

1 km   N

c

31°47' N
55°58' E

N

500 m
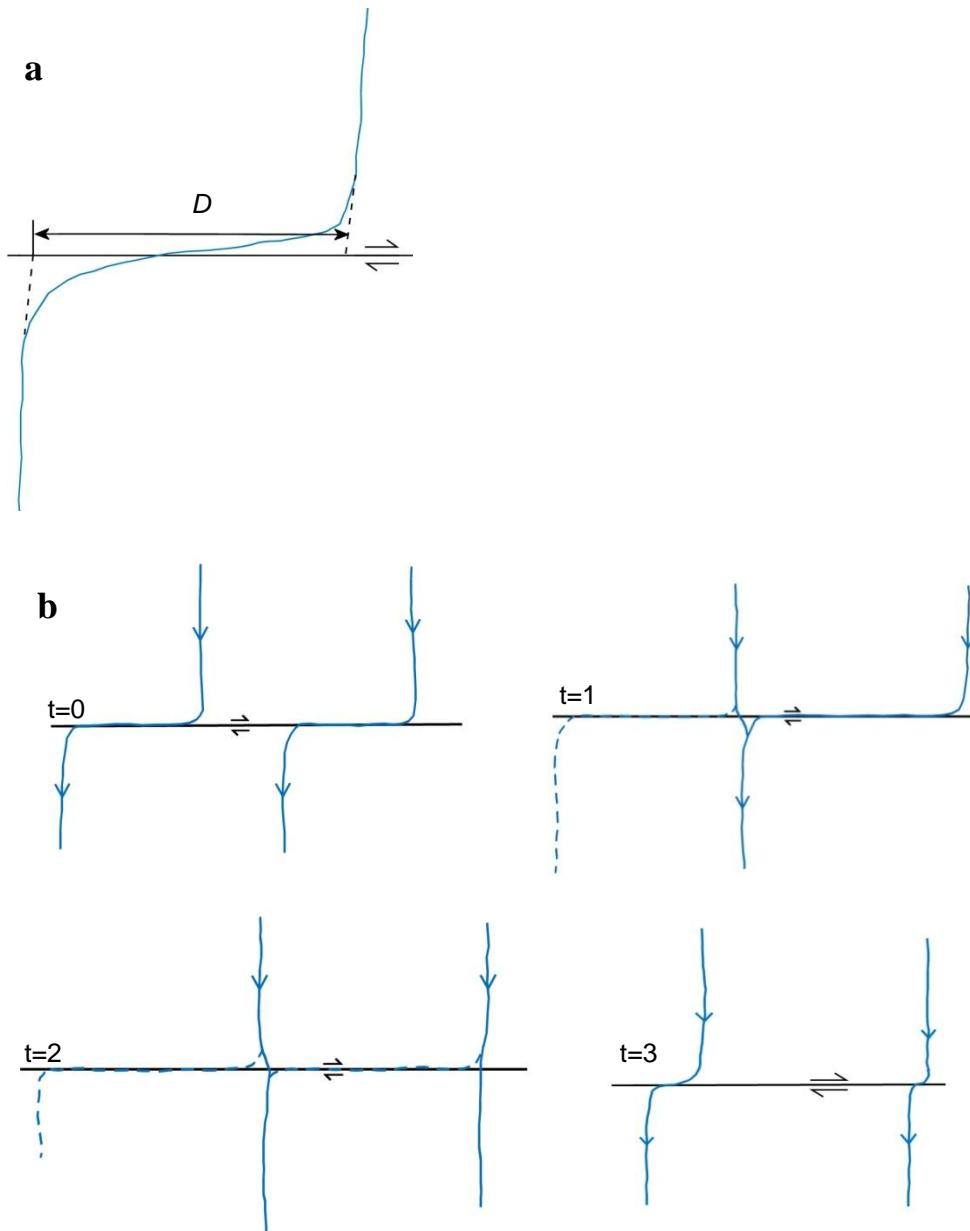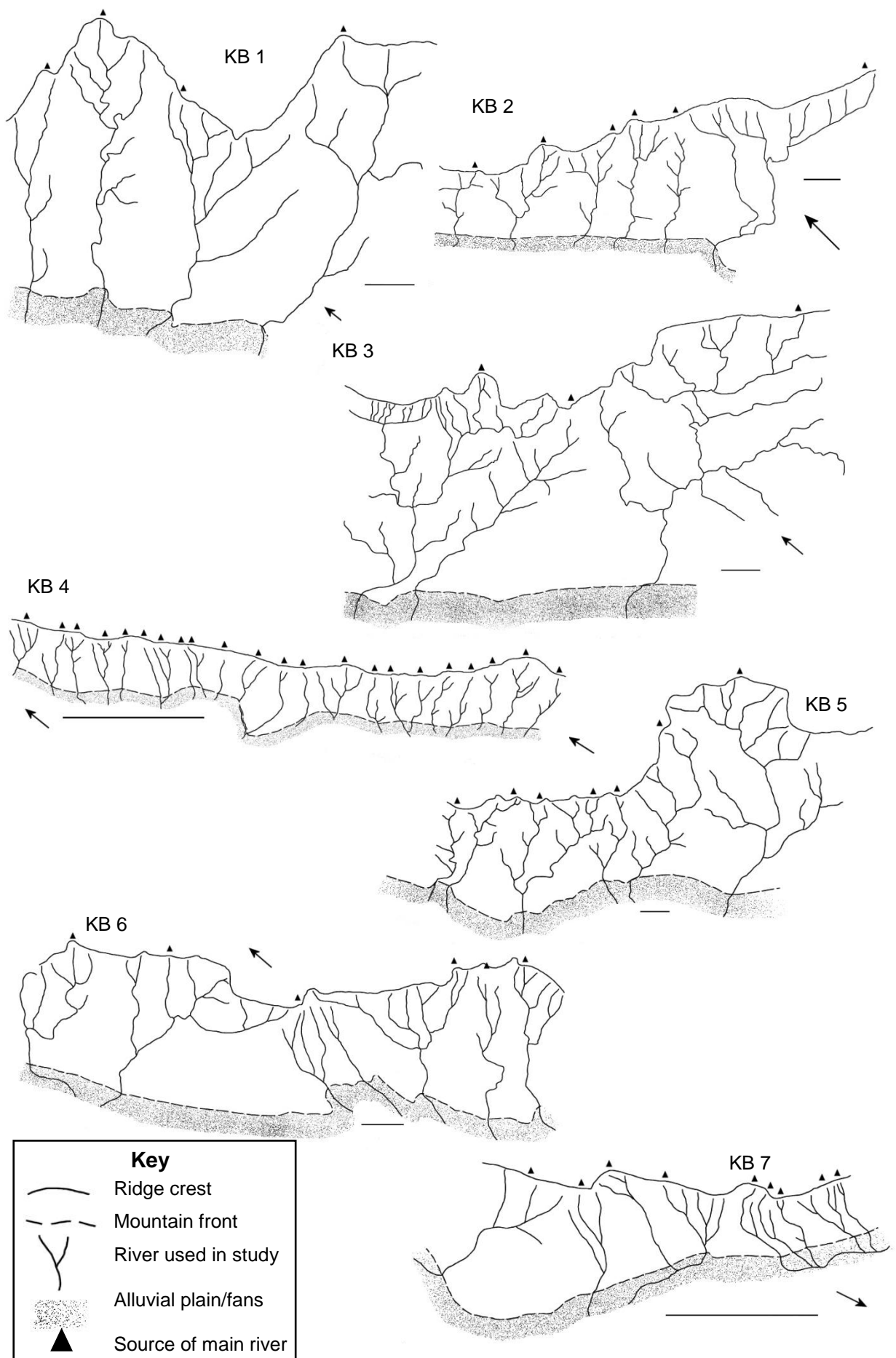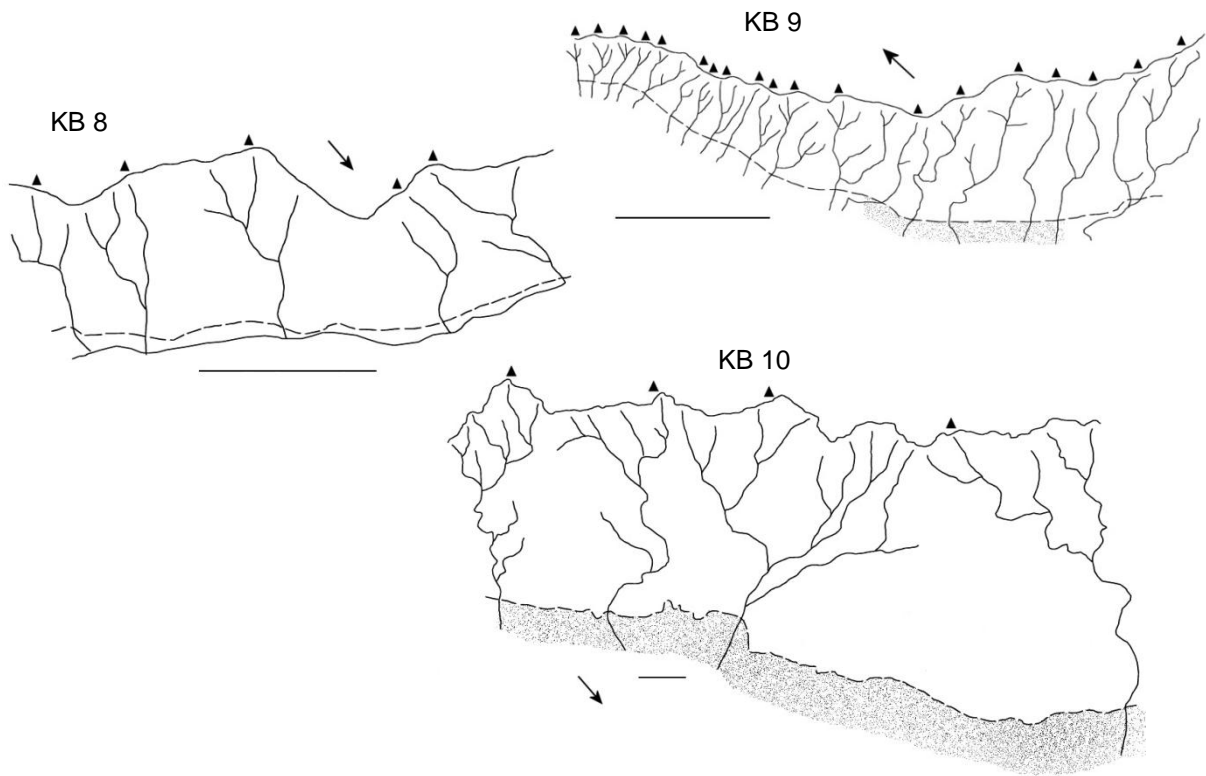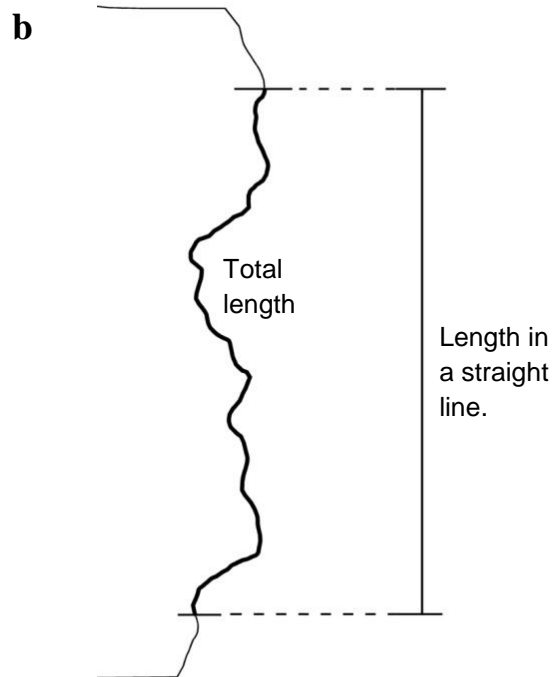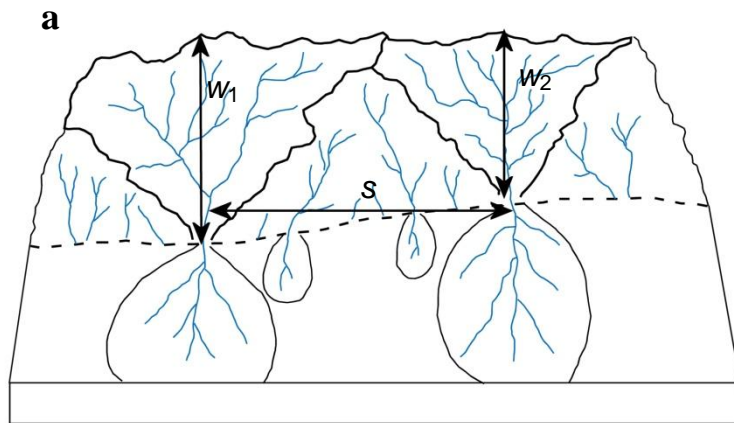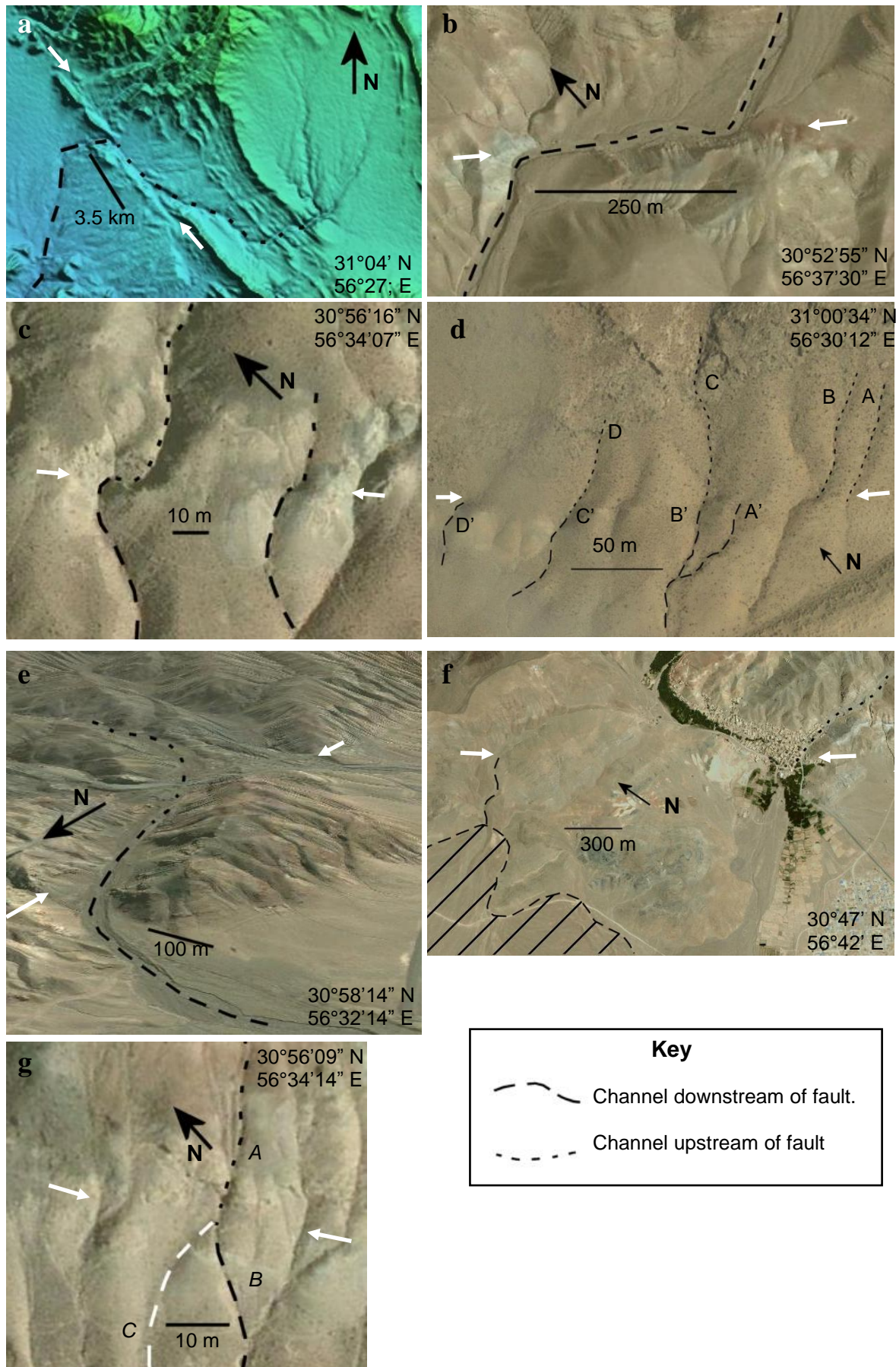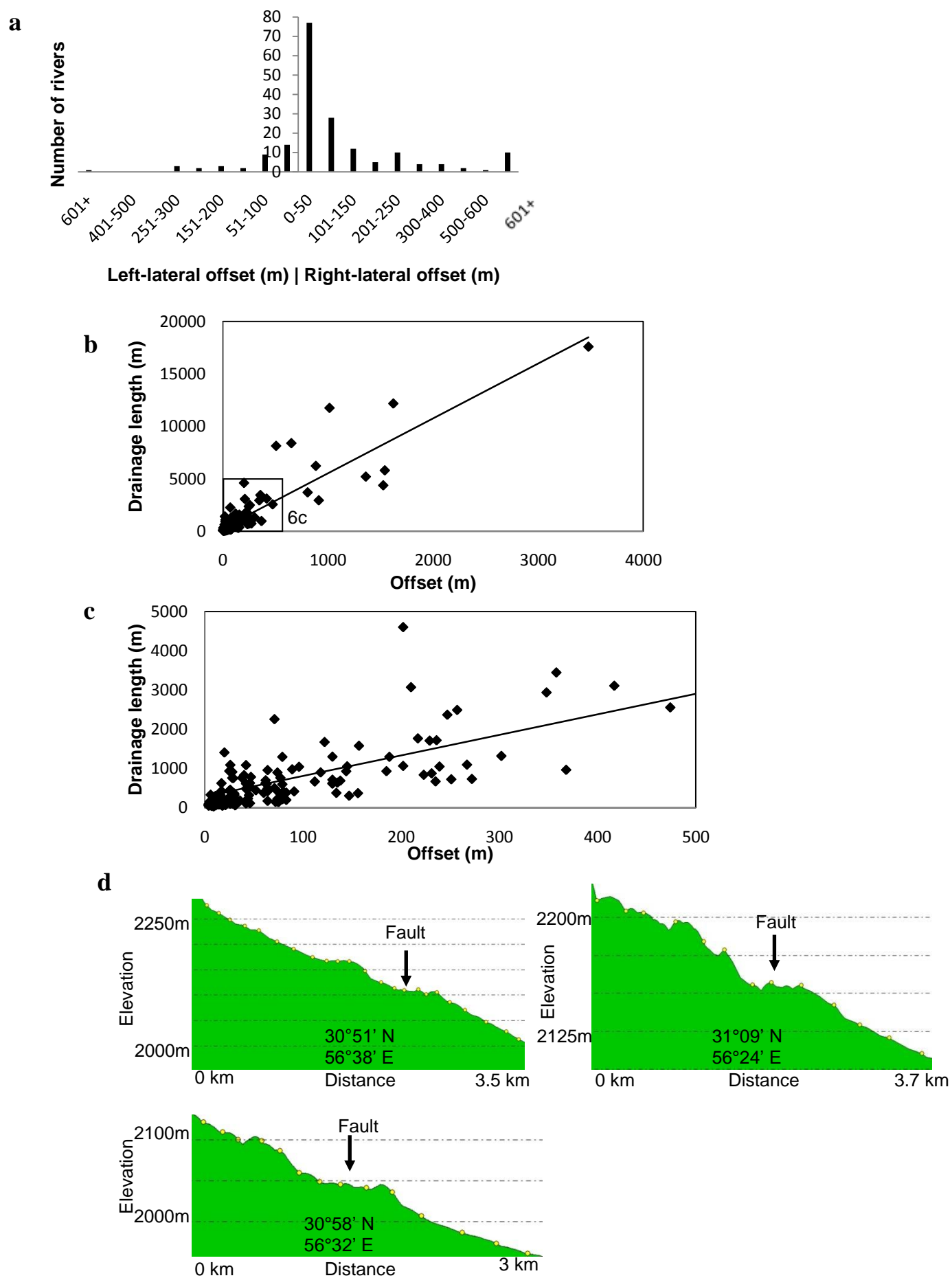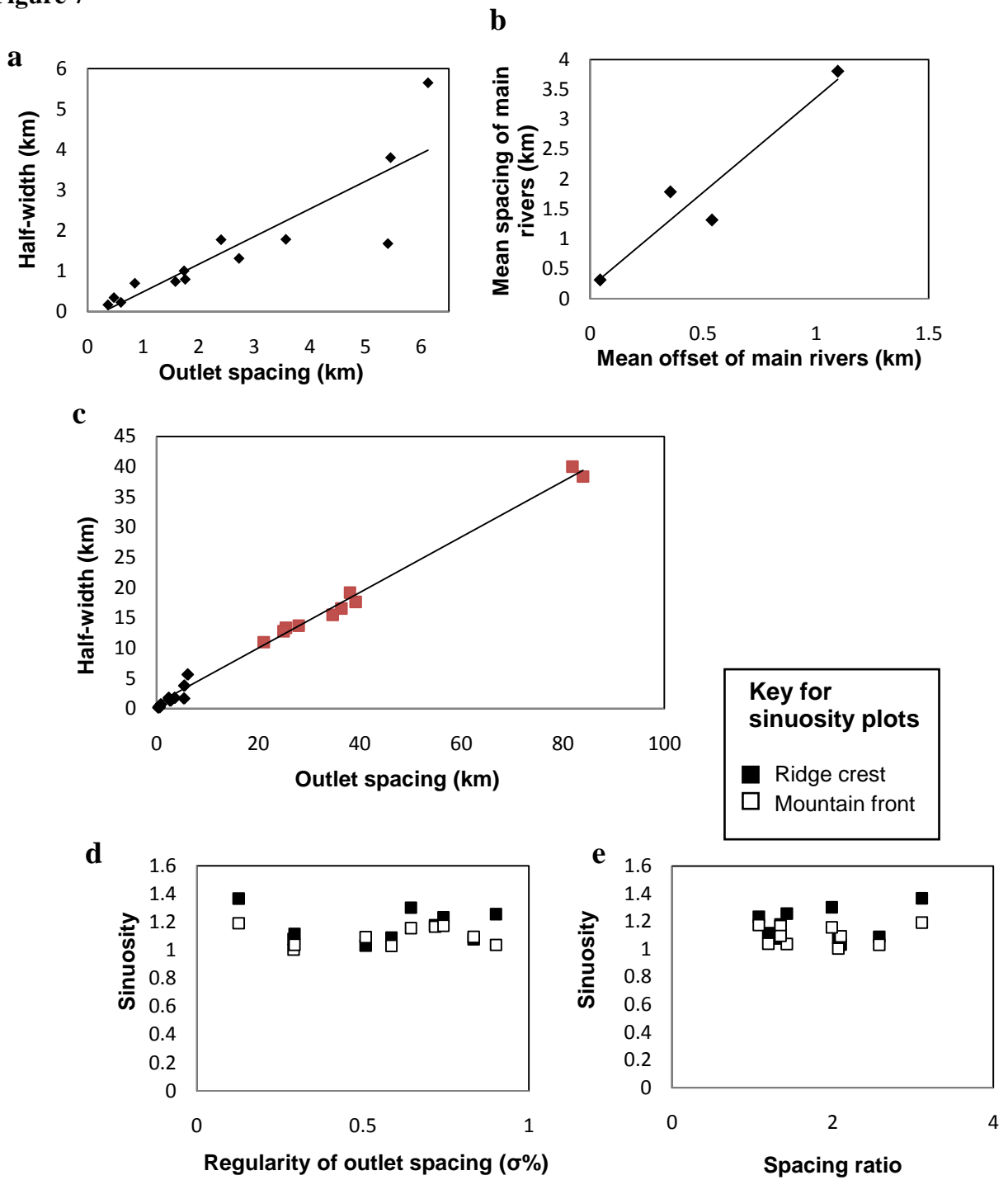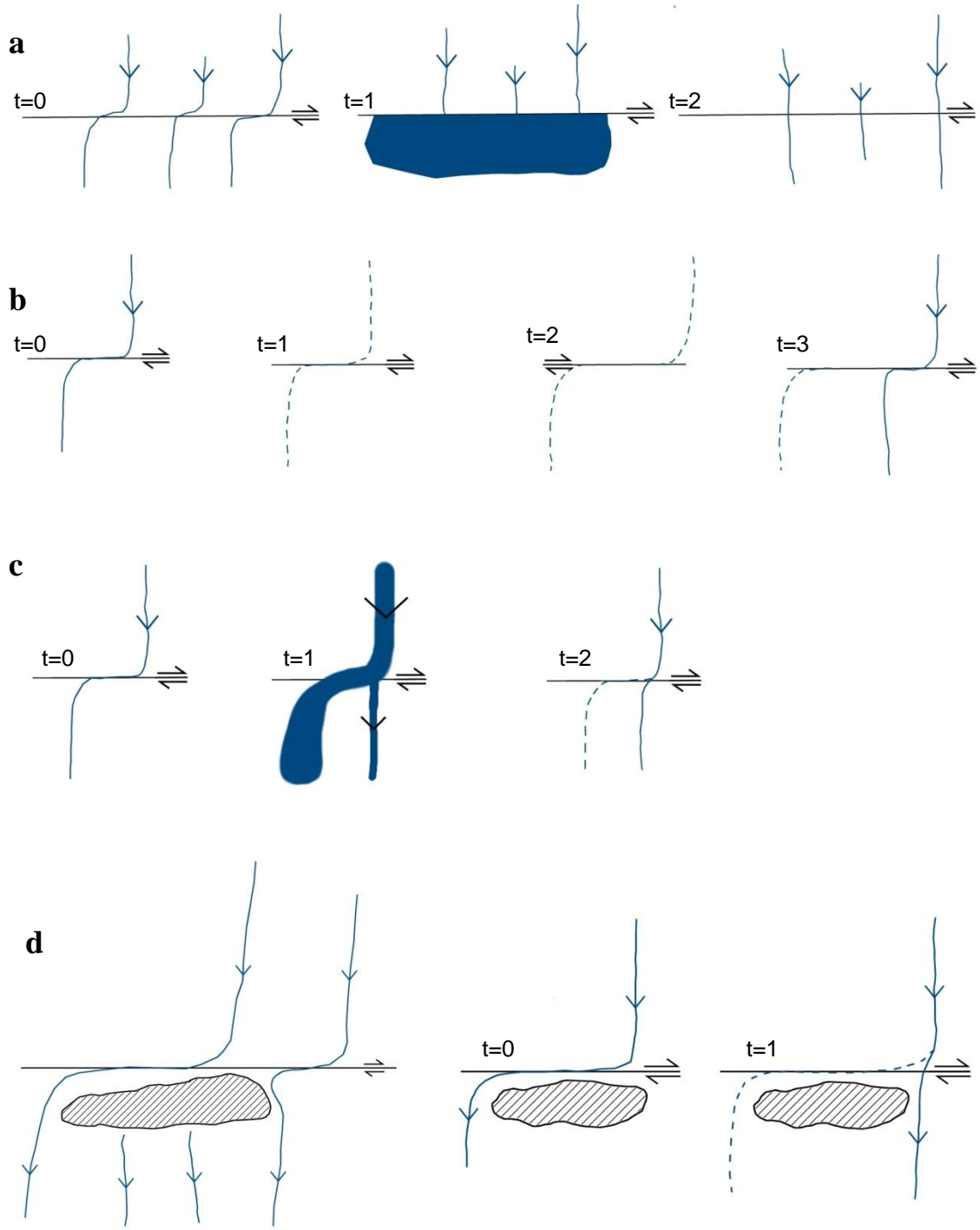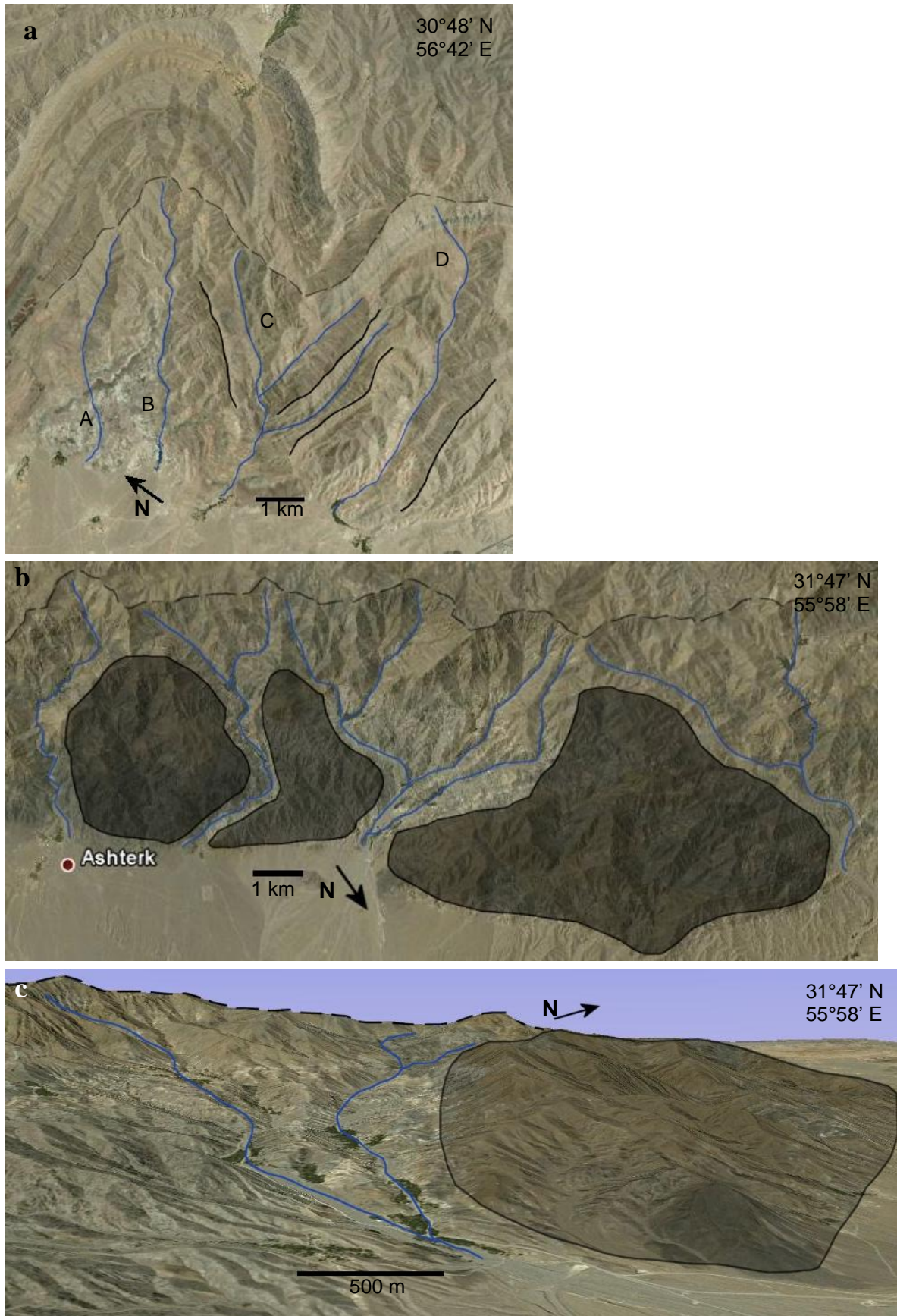
Figure 10
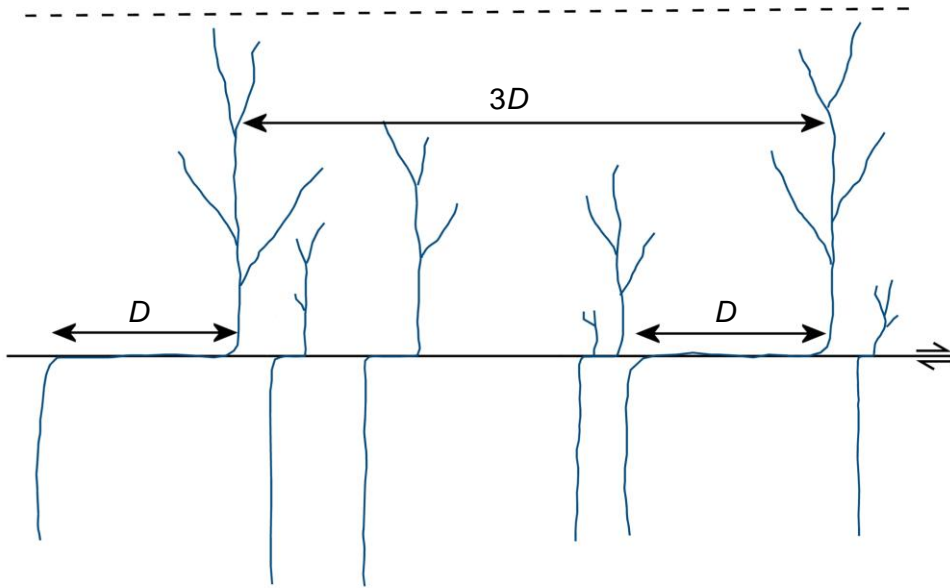
Supplementary material for online publication only
Click here to download Supplementary material for online publication only: Appendices 1&2.docx